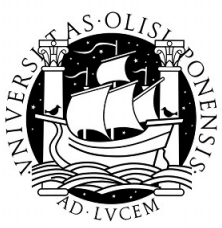


UNIVERSIDADE DE LISBOA

FACULDADE DE CIÊNCIAS

DEPARTAMENTO DE ENGENHARIA GEOGRÁFICA, GEOFÍSICA E ENERGIA

# Wave Propagation in the Portuguese Nearshore, with Application to Wave Energy Resource Assessment

Marco Miani

**Mestrado em Ciências Geofísicas**
**Especialização em Oceanografia**

2009

UNIVERSIDADE DE LISBOA

FACULDADE DE CIÊNCIAS

DEPARTAMENTO DE ENGENHARIA GEOGRÁFICA, GEOFÍSICA E ENERGIA

# Wave Propagation in the Portuguese Nearshore, with Application to Wave Energy Resource Assessment

Marco Miani

**Mestrado em Ciências Geofísicas**
**Especialização em Oceanografia**

**Trabalho de Projecto orientado**
**pelo Professor Joaquim Dias e pela Doutora Teresa Pontes**

**2009**

**Abstract**

SWAN wave model (Simulating Waves Nearshore, TU Delft) has been validated against in situ observations for two months: October and June (wave climate) analyzing salient wave parameters ($H_s$, $T_e$, $\Theta$ and Energy Flux (P) ) for the Portuguese Pilot Zone (PZ). The model slightly over predicts $H_s$, while $T_e$ is underestimated. Energy Flux (P) also shows mis estimation. $\Theta$ is well predicted. Mis estimation is certainly due to improper boundary conditions (WAM 2D spectra).
Extreme (stormy) observed sea states, typical for winter, are mis predicted by wave model; milder condition, typical in summer, are better predicted but still some important differences are observable.

**Key-words**: SWAN wave model, underestimation, energy period

**Resumo**

Portugal tem um recurso de energia das ondas de aproximadamente 25 a 30 kW/m, sendo a costa NW o local mais vantajoso em termos de potência disponível. O recurso total médio foi estimado em 10 GW podendo ser metade deste potencialmente utilizado [Clément et al., 2002].
O objectivo principal desta tese de mestrado, é o estudo dos parâmetros de ondulação para a Zona Piloto (ZP) Portuguesa, com a finalidade de avaliar o recurso energetico para aquela zona. Em particular foram tidos em consideração dois meses: Outubro e Junho de 2008. Estes meses, situados, respectivamente, no inverno e verão, fornecem-nos uma indicação do clima de ondas na zona piloto para estas estações. O mês de verão apresenta um perfil energético menos intenso (entre 10 e 40 kW/m) relativamente ao mês de inverno (com valores bastante mais elevados podendo ultrapassar os 120kW/m para tempestades). Os parâmetros espectrais objecto deste estudo são a altura significativa ($H_s$=$4\sqrt{m_0}$) e o período de energia ($T_e = m_{-1}/m_0$). É de salientar que a potência transportada pelas ondas está directamente relacionada com estes dois parâmetros para águas profundas ($P = 0.49 \times H_s{}^2 T_e$). Com o fim de validar a qualidade dos resultados obtidos, calculam-se os seguintes parâmetros de estatística de erro: $E_{rms}$, Viés, Scatter Index. Este estudo segue o estudo análogo, apresentado em [Bruck et al., 2009], que utilizou como forçamento na fronteira os espetros do modelo de ondas MAR3G [Pires, 1993] actualmente utlizado no Instituto de Meteorologia Português. Foi decidido estudar este caso porque em [Bruck et al., 2009] o período de energia ($T_e$) é sensivelmente sub-estimado, enquanto os outros parâmetros espectrais apresentam uma concordância melhor, quando confrontados com os dados da bóia medidos na Zona Piloto. A direcção da ondulação (direcção média por banda de frequência: $\bar{\theta}$) também é estudada. Observou-se que as ondas usualmente vêm de NW, de acordo com o campo de ventos. Os parâmetros de ondulação marítima foram obtidos a partir de dados da bóia estação ondografo direccional instalada ao largo de S. Pedro de Moel. A estação é composta por uma bóia *DIRECTIONAL WAVERIDER*, e esta situada na posiçao latitude=39° 53' 00"N, longitude=, 09° 04' 04"W, a uma profundidade de 50.5 metros. Os dados constituidos por seriés temporais de deslocamento vertical (elevações) e horizontais segundo os eixos N-S e E-W, sao calculados pelo microprocessador instalado na bóia, a partir das medições das tres componentes de acceleração do movimento da superfície livre

e das três componentes do campo magnético terrestre. Em condições normais a aquisiçao dos dados é efectuada de três em três horas, durante períodos de 30 minutos. Em condições de temporal, ou seja, quando a altura significativa excede os 5 metros, os períodos de aquisição são de 30 minutos apenas espaçados de pequenos intervalos necessários ao processamento dos dados. Os dados são adquiridos a uma taxa de digitalização de 1.28 amostras por segundo (1.28 Hz) e agrupados em blocos de 200 segundos. O limite mínimo de duração para que um conjunto de dados (registo) seja tratado é de 10 minutos. Os grupos data-hora estão referidos á hora local e correpondem ao início dos registos. Os dados foram processados tendo em vista as estimativas da distribuição de energia, direcção média e dispersão, por bandas de frequência, bem como a estimação dos parâmetros característicos da agitação, no que respeita a alturas, períodos e direcções. As séries temporais de elevação foram também processadas pelo método directo. Neste trabalho utiliza-se dois modelos numéricos espectrais de terceira geração , SWAN [Booij et al., 1999] e o MAR3G [Pires, 1993] utilizado actualmente pelo Instituto de Meteorologia Português. O SWAN (Simulating WAves Nearshore) é um modelo, que permite obter estimativas dos parâmetros espectrais da agitação marítima em áreas costeiras, lagos e estuários, tomando em consideração a batimetria e os campos de correntes e ventos. Conceptualmente, trata-se de um modelo de geração, propagação e dissipação da agitação marítima, baseado na equação de conservação da acção de onda. O SWAN tem implementado os processos físicos presentes na propagação da agitação, nomeadamente, refracção devido a variações do fundo e á presença de correntes, interacção onda-corrente, reflexão/transmissão através de obstáculos, interacções não-lineares entre ondas, crescimento de onda por acção do campo de ventos e dissipação de energia devido ao atrito do fundo e à rebentação tanto por influência do fundo como por excesso de declividade (*whitecapping*). A propagação da agitação é realizada utilizando esquemas numéricos implícitos (*Backwarded in Time, Backwarded in Space*, BSBT), podendo-se utilizar coordenadas cartesianas ou esféricas. O modelo pode ser executado em modo estacionário ou não estacionário. Os dados do modelo SWAN são, basicamente, o espectro a propagar ,a malha de diferenças finitas em que é discretizada a região em estudo e as opções de cálculo. O modelo calcula o espectro direccional em cada ponto do domínio. Assim, é possível obter-se valores para a altura significativa, período de energia e direcções médias espectrais. O modelo SWAN é utilizado para estudar a ZP (tal como mostrado em Fig. 3). A batimetria, fornecida pelo Instituto Hidrografico, tem uma resoluçao (igual em -x e em -y) de 18 segundos de arco (aproximativamente 556 metros), tal como mostrado na Fig. 2. Os dados de imput para o SWAM são os espectros direccionais na fronteira do domínio e o campo de ventos. O campo do vento (a 10 metros de altura), calculado pelo modelo MM5 ([Grell et al., 1994]), tem uma resolução espacial de 5 km e um passo no tempo de 6 horas. Sendo o campo de vento definido em coordenadas UTM (*Universal Transversal Mercator*), e não sendo a malha para o campo de vento igualmente espaçada, foi necessário interpolar o campo de vento originalmente calculado pelo MM5 e definir, dessa forma, uma grelha estruturada e igualmente espaçada facilmente assimilável pelo modelo de ondas SWAN. Para confirmar que o modelo assimilava bem os dados, foram sobrepostas a séries temporais de entrada (modelo MM5) e de saída (produzida pelo SWAN) da intensidade do vector do vento ($\|\vec{v}\|$) para as cordenadas correspondentes á posição da bóia. O resultados mostram uma correspondencia excelente (Figura 11), sugerindo que a assimilação è correctamente efectuada.

Por além de isto, é de notar que os picos no campo do vento ($\|\vec{v}\|$) devidos a tempestades, estão correlacionados com os picos de altura significativa ($H_s$). Da mesma maneira, $H_s$ diminui quando $\|\vec{v}\|$ diminui.

Os espetros na fronteira são bidimensionais (direccionais) mês de Junho e Outubro, fornecidos pelo modelo de ondas WAM [Group, 1988], tendo 30 frequências (logaritmicas ) e 24 direcçoes (igualmente espaçadas). As fronteiras do domínio computacional foram forçadas, respeitavemnte, com 2 (SUL), 3 (OESTE) e 3 (NORTE) espectros. O comprimento de cada cada fronteira (SUL, OESTE e NORTE) foi dividido pelo número de espectros a aplicar naquela fronteira (subsegmento) e, nos cantos do domínio (rectângulo), o mesmo espectro foi prescrito para ambos os sub-segmentos. Por além dos espetros na(s) fronteira(s), há também um espetro WAM bidimensional que se localiza perto da bóia (cerca 15 km de distância) e encontra-se numa posição em que água tem uma profondidade de 36 metros. O modelo subestima sensivelmente o período de energia ($T_e$) tal como a altura significativa, embora esta seja melhor estimada. A subestimaçao é devida ás condições utilizadas para forçar o modelo: analizando as séries temporais, o período de energia ($T_e$) do WAM é muito baixo. Analizando a forma espectral para cada passo de tempo (3 Horas) nota-se que, para o modelo WAM forçado a ser propagado), as altas frequências apresentam densidades espectrais irrealisticamente altas. Isto faz com que o período de energia tenha tendência a ser mais baixo Em respeito às alturas significativas, os valores (numéricos) observados e simulados apresentam uma concordância melhor, embora exista ainda uma ligeira discrepância, especialmente para as condições de agitação marítima mais intensas (tempestade e inverno). O modelo WAM não consegue resolver bem os estados do mar mais energéticos: em condições de baixa energia (ondulaçao moderada) a discrepância é menor, se for confrontada com a discrepância observada em condições de agitação muito intensa (por ex: bóia mede 32 $m^2$/Hz, o modelo prevê 5 $m^2$/Hz) para qualquer gama de frequências. Deduz-se que os resultados não são satisfatórios, devido ao facto das condições prescritas na fronteira do modelo SWAN nao serem adequadas. Para além do modelo de ondas SWAN, outro modelo foi utilizado para avaliar o recurso energético das ondas: trata-se do modelo de terceira geraccão MAR3G [Pires, 1993]. Os espectros bidimensionais (direccionais) calculados pelo MAR3G têm 25 frequências (logarítmicas) e 24 direcções (igualmente espaçadas), sendo logo possivel calcular os parâmetros tipicos ($H_s$, $T_e$. $\bar{\theta}$, P) e confrontá- los com o modelo WAM. Tal como descrito em [Bruck et al., 2009], o período de energia estimado por este modelo também é subestimado (às vezes sensivelmente) enquanto a altura parece mostrar uma melhor concordância. O modelo MAR3G é actualmente utilizado para a previsão operacional pelo Instituto de Metereologia Portuguesa. Dois pontos do MAR3G foram comparados com dois pontos do WAM. No primeiro caso, ambos os pontos (Figueira da Foz para o M3G e S17NN para o WAM) tinham as mesmas coordenadas (41N, 9W), e para aquelas coordenadas a água tem uma profundidade de 82 metros. No segundo caso, os pontos são Peniche para o MAR3G e S7 para o WAM e as coordenadas são respectivamente 39°N, 10°W (profundidade = 245 metros) e 39°N, 9.5°W (profundidade = 55 metros). Tal como no caso do WAM, os espectros do MAR3G apresentam uma densidade espectral irrealista nas altas frequências. O efeito é o mesmo descrito para o caso anterior.

Palavras chave: energia das ondas, modellação numerica, Zona Piloto.

# Acknowledgments

Many thanks to Dr. **Maria Teresa Pontes** (principal researcher at *I.N.E.T.I.*), who supervised and encouraged me during elaboration of the present work.

I would also like to express my appreciation to my supervisor: Prof. **Joaquim Dias** (*Instituto de Oceanografia* - Faculty of Science - University of Lisbon) for his guidance, support and his lectures in *Oceanografia Costeira*.

To Dr. **Paulo Justino** (modeller and researcher at *I.N.E.T.I.*) I would like to express my sincere gratitude: thank you for your precious support, advices, and helping me to getting the wave model working.

Also, special thanks to Christian Feuersänger, Institut für Numerische Simulation, Universität Bonn, Germany for helping me with issues related to LaTeX code.

This work would not have been completed without help and support of many individuals. I would like to thank everyone who has helped me along the way. Especially, I would like to thank and hug Hugo, Petra, Daniel, Hector and Oscar for cheering me up during the difficult times and the nice moments we spent at the beach, playing Frisbee.

*Martifer* Group kindly provided wave in situ data (buoy measurements) at the Portuguese Wave Energy Pilot Zone for months of June and October 2008.

# Contents

# List of Figures

# List of Tables

# Simulating Waves in Nearshore Areas - The Portuguese Pilot Zone

This part is devoted to describe the methodology, as well as the results obtained by employing SWAN wave model for the area of interest (Pilot Zone), and validating it against *in situ* observations for two months: June and October 2008. After briefly introducing (a) the area of study and (b) observed data, obtained results are described in detail in sections 4 and 8.

## 1 SWAN model description

For this investigation, SWAN wave model is used [Booij et al., 1999], version 40.72. It is a third-generation wave action model designed to resolve wave fields in shallow waters, such as coastal regions. It uses typical formulations for wave growth by wind, wave dissipation by white-capping, and four wave nonlinear interactions (quadruplets). It also includes physical processes (e.g., bottom friction) that are not pertinent to the cases of the present study. The governing equation of SWAN and other third generation wave action models is the action balance

$$\frac{\partial N(\sigma,\theta,x,y,t)}{\partial t}+\frac{\partial c_{g,x}N(\sigma,\theta,x,y,t)}{\partial x}+\frac{\partial c_{g,y}N(\sigma,\theta,x,y,t)}{\partial y}+ \\ +\frac{\partial c_{g,\sigma}N(\sigma,\theta,x,y,t)}{\partial \sigma}+\frac{\partial c_{g,\theta}N(\sigma,\theta,x,y,t)}{\partial \theta}=\frac{S_{\mathrm{tot}}}{\sigma}. \quad (1)$$

where $\sigma$ is the relative (intrinsic) frequency (the wave frequency measured from a frame of reference moving with a current, if a current exists); N is wave action density, equal to energy density divided by relative frequency (N = E/$\sigma$); u is wave direction; $c_g$ is the wave action propagation speed in $(x, y, s, u)$ space; and S is the total of source/sink terms expressed as wave energy density. For this special case of study, the right-hand side of (1) is dominated uniquely by $S_{in}$: wind generation (always positive source term) which will be briefly discussed here.

### 1.1 Wind Input

According to [Miles, 1957], wind growth might be physically described as follows:

$$S_{in}(f,\theta)=\alpha+\beta E(f,\theta). \quad (2)$$

The coefficient $\beta$ depends on the speed and direction of the wind ($\theta_{wind}$) and the wave ($\theta$): $\beta \sim$ [U cos($\theta$-$\theta_{wind}$)/c]$^2$, where U is a reference wind speed (not necessarily $U_{10}$) and $c$ is the phase speed of the water-wave component. Different wind-schemes are available; the one used here (default) is Komen's [Komen et al., 1994].

$$\beta=\max[0,0.25\frac{\rho_a}{\rho_w}(28\frac{U_*}{c_{\mathrm{ph}}}\cos(\theta-\theta_w)-1)]2\pi f \quad (3)$$

# 2 Metodology

## 2.1 Objective

The main goal of this Master Thesis is to study wave energy resource at the Portuguese Wave Energy Pilot Zone. The study is made using SWAN model to propagate the wave conditions offshore that are computed by the well-known WAM [Group, 1988] numerical wind-wave model running at the European Centre for Medium-Range Weather Forecast [ECMWF]. This study follows a similar one [Bruck et al., 2009] that used as boundary conditions the results of the MAR3G model [Pires, 1993] that is run at the *Insituto de Meteorologia* of Portugal. The reason why it was decided to perform the present study is because of the wave period was too low, while the other wave parameters fitted reasonably buoy data measured at the Pilot Zone in order to assess wave energy resource. Suitability of numerical wave models, employed for the scope, is taken into consideration.
MAR3G (M3G) model was used (as reported in [Bruck et al., 2009]) on boundary conditions for SWAN model. However it was found that (SWAN $T_e$ values did not fit well buoy data), the fitting of M3G results to buoy data was not good (model underestimated energy period). As reported in [Bruck et al., 2009], in fact, the problem to overcome is the improvement of boundary conditions (especially energy period, $T_e$ also under predicted).

## 2.2 Problem Statement

This will deal with the quality of performances of SWAN wave model when simulating representative wave parameters such as (but not only) Energy Period ($T_e$) and Significant Wave Height ($H_s$).
In order to obtain more realistic boundary conditions for the SWAN computations in the Pilot Zone (see Figure 3) results of ECMWF WAM model were obtained and used.

## 2.3 Modus Operandi

In order to study these discrepancies, it is therefore important to compare M3G and WAM results and, for a location close to the buoy site, compare also those results to the buoy data. Such comparison will be present graphically and numerically (using typical error statistic indicators: $E_{rms}$, Bias, Scatter Index) for both months. Ocean waves, and therefore the sea-sate, is described through two-dimensional spectra.

> The aim of describing ocean waves with a spectrum is not so much to describe in detail one observation of the sea surface, but rather to describe the sea surface as a stochastic process, i.e., to characterize all possible observations (time records) that could have been made under the conditions of the actual observation. An observation is thus formally treated as one realisation of a stochastic process. Here, we base this treatment on the random-phase/amplitude model, which leads to the wave spectrum, which is the most important form in which ocean waves are described [Holthuijsen, 2007]

Let $m_n$ be the $n-th$ spectral moment:

$$m_n = \int_0^{2\pi} \int_{f_{min}}^{f_{max}} f^n \, S(f,\theta) \, df d\theta. \tag{4}$$

One-dimensional spectrum (S($f$)) or D($\theta$) are obtained from bi-dimensional (S($f,\theta$)) spectrum:

$$S(f) = \int_0^{2\pi} S(f,\theta) \, d\theta; \quad D(\theta) = \int_{f_{min}}^{f_{max}} S(f,\theta) \, df. \tag{5}$$

Wave parameters are, thus, easily defined as:

1. **Significant Wave Height** ($H_S$ or $H_{m0}$), calculated after retrieving $m_0$: the zero-th spectral moment

$$H_s = 4\sqrt{m_0} \tag{6}$$

2. **Energy Period** ($T_e$ or $T_{m-10}$). This parameter was not directly available: I have been calculating it after retrieving involved spectral momenta ($m_{-1}$ and $m_0$). According to [Holthuijsen, 2007], energy period $T_e$ is defined as:

$$T_{m-10} = \frac{m_{-1}}{m_0} \tag{7}$$

3. **Mean wave direction**[1]. This quantity, $\bar{\theta}$, was distributed as a function of frequency:

$$\bar{\theta}(f); \quad \sigma_\theta(f)$$

where $\sigma_\theta(f)$ is the associated standard deviation.

$$\bar{\theta} = \arctan \left\lfloor \frac{\int\int \sin\theta E(f,\theta) df d\theta}{\int\int \cos\theta E(f,\theta) df d\theta} \right\rfloor \tag{8}$$

4. **Power**, or Energy Flux (P) per unit wave front has been obtained by following integral:

$$P = \rho_w g \int_0^{2\pi} \int_{f_{min}}^{f_{max}} S(f,\theta) \cdot c_g(f,d) \, df d\theta \tag{9}$$

where: $\rho_w$ is water density (1025 kg/m$^3$), g is gravitational acceleration (9.81 m/$s^2$) and $c_g(f,d)$ is wave group celerity (for each frequency $f$ at depth $d$). For the case of buoy data (one-dimensional spectra) Equation 9 becomes a single integral in S($f$) (see Equation 5) .

[1]Formerly not nautical but converted so in order to be consistent with wave model results.

### 2.3.1 Error statistics

For a further stage, it shall be necessary to numerically define quality standards: in fact, to quantify model's performance, a set of convenient parameters has been defined:

1. **Root Mean Square Error** ($E_{rms}$):

$$E_{rms} = \sqrt{\overline{(X_{Obs} - X_{Sim})^2}} \tag{10}$$

2. **Bias**:

$$Bias = \bar{X}_{Obs} - \bar{X}_{Sim} \tag{11}$$

3. **Scatter Index** (S.i.), defined as the $E_rms$ normalized with the mean observed value:

$$S.i. = \frac{E_{rms}}{\bar{X}_{Obs}} \tag{12}$$

# 3 Introduction

## 3.1 Area of Interest

The area under study, i.e. where SWAN model has been run for, is shown in Figure 1: it is approximately a 55×55 km$^2$ square. The bathymetry, represented in Figure 2, ranges from 0 to 160 meters water depth.

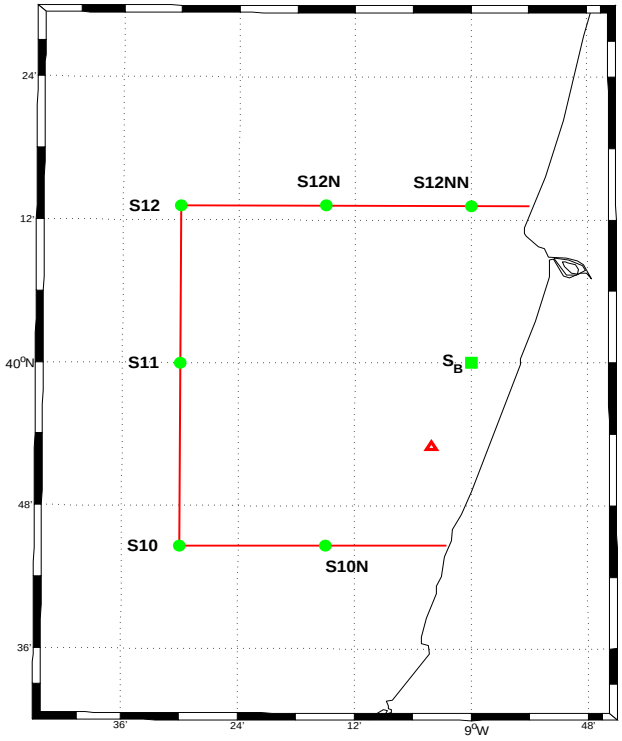


Figure 1: The box delimits the area under study. Circles represent location where boundary conditions are prescribed (with names); another directional WAM spectrum is located near buoy site: "$S_B$" (marked with a rectangle). The triangle spots the buoy site. The box also coincides with limits of the bathymetric and computational grid.

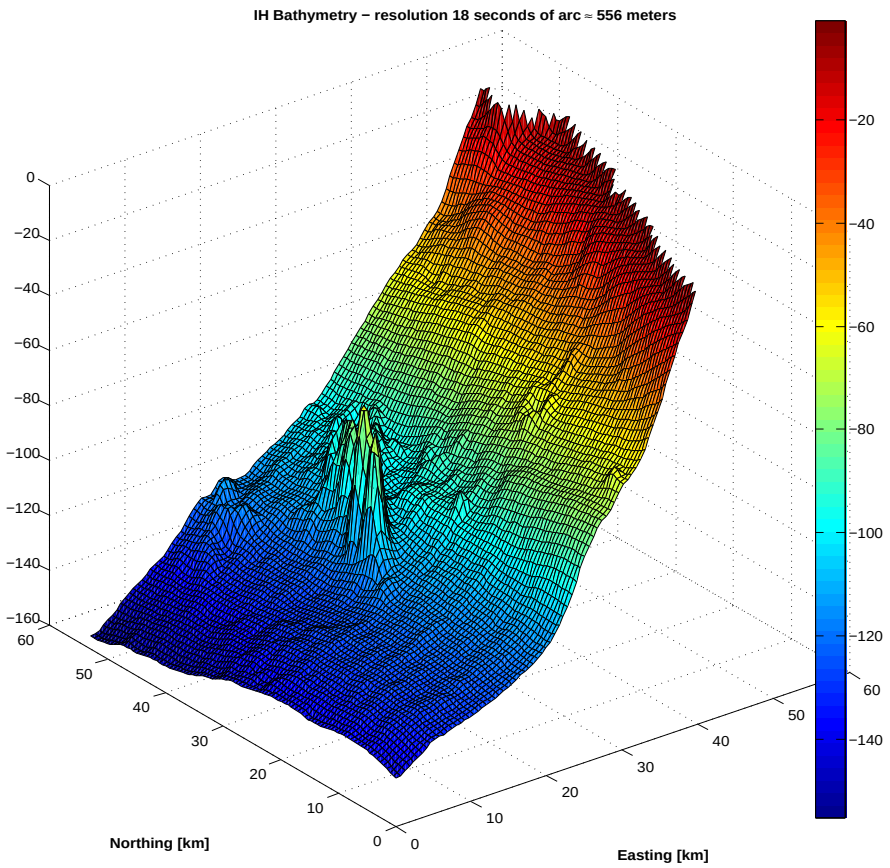


Figure 2: 3D plot of the bathymetry, in the area of study as shown in Figure 1, framed into problem co-ordinates and showing a quasi regular profile. The mesh has 99 and 95 nodes respectively in x- (i.e. East-West) and y- (i.e. North-South) directions. Point (0,0) has co-ordinates 39°44'38.85"N 9°30'0.19"W (see Figure 1).

Bathymetric data have been provided by *Instituto Hidrografico* (IH): the Portuguese Hydrographic Institute. The mesh has a resolution of 18 seconds of arc that correspond to about 556 meters (both for x- and y- direction). The total bathymetric data span from: $9.5°W$ to Coast and $38.5°N$ to $40°N$; see Figure 1.

Figure 2 presents the 3D bathymetry plot framed in **problem coordinate system**: water depth is given in meters. The origin of this reference frame, whose co-ordinate are $(0, 0)$, coincides with bottom left (South-West) corner of the mesh, (Figure 1).

## 3.2 Pilot Zone

The Pilot Zone (Figure 3) is bounded between following coordinates :

- 39° 57' 30"N and 9° 0' 5.42"W
- 39° 57' 30"N and 9° 12'W
- 39° 47' 30"N and 9° 12'W
- 39° 47' 30"N and 9° 3' 53.20"W

Eastern limit corresponds with 30 meters isobath line.

# 4 Data Set

## 4.1 Waverider Buoy

Wave measurements in the Pilot Zone were made by a DIRECTIONAL WAVERIDER. It is a spherical, 0.9 m diameter, buoy which measures wave height and wave direction. The direction measurement is based on the translational principle which means that horizontal motions instead of wave slopes are measured. As a consequence the measurement is independent of buoy roll motions and therefore a relative small spherical buoy can be used. A single point vertical mooring ensures sufficient symmetrical horizontal buoy response also for small motions at low frequencies [Datawell].
Wave buoy is moored at 39°53'00"N, 9°04' 04"W (WGS 84) where water is 50.5 meters deep. Sample frequency is 1.28 Hz.
Furthermore:

- number of frequency bins: 127,
- frequency range: [$f_{min}$=0.005 H, $\Delta f$ = 0.005 Hz, $f_{max}$=0.635 Hz]
- sampling interval ($\Delta t$) = 3 hours,
- directional information[2] is provided as mean wave direction per frequency band ($\bar{\theta}(f)$) and the respective standard deviation ($\sigma_\theta(f)$)

Two months have been used as a first step for validation of SWAN results for the Pilot Zone: **June and October** ( 2008). These months have been chosen to study difference between winter and summer wave climate conditions.

## 4.2 Wave Data

### 4.2.1 June 2008

As showed in following plots, wave parameters portrait milder conditions for this summer month. Wave height is smaller, barely exceeding 2 meters, as expected. Wave period, bounded between 5 and 10 seconds, shows a typical wind sea profile. Confront with Figures 25 to 27, in section 8.1.

[2]Buoy's directions are provided according to *cartesian* convention.

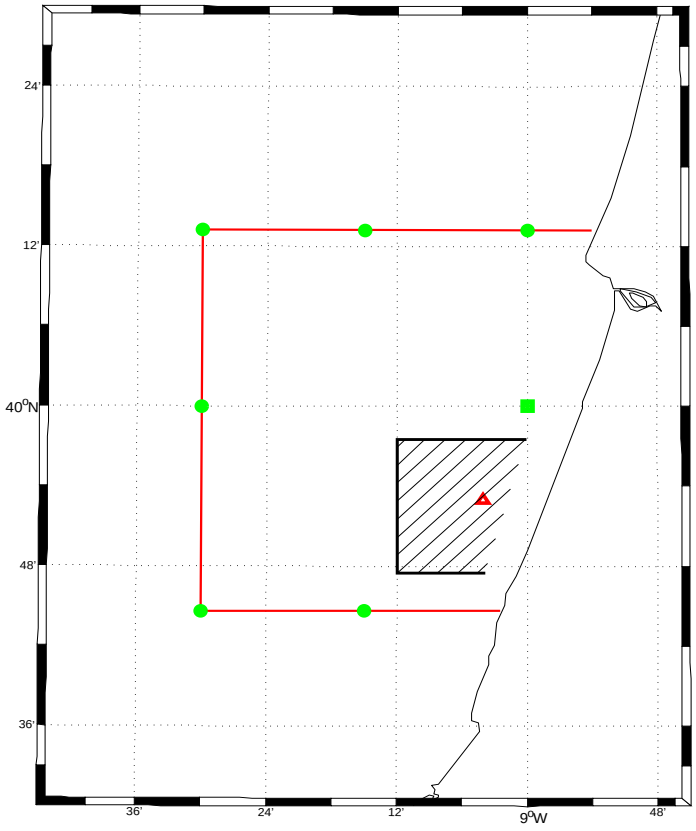


Figure 3: Representation of the Wave Energy Pilot Zone (shadowed in black) framed into area of interest and bounded on the east by the 30-meters contour line. Boundary conditions (dots) represented as in Figure 1.

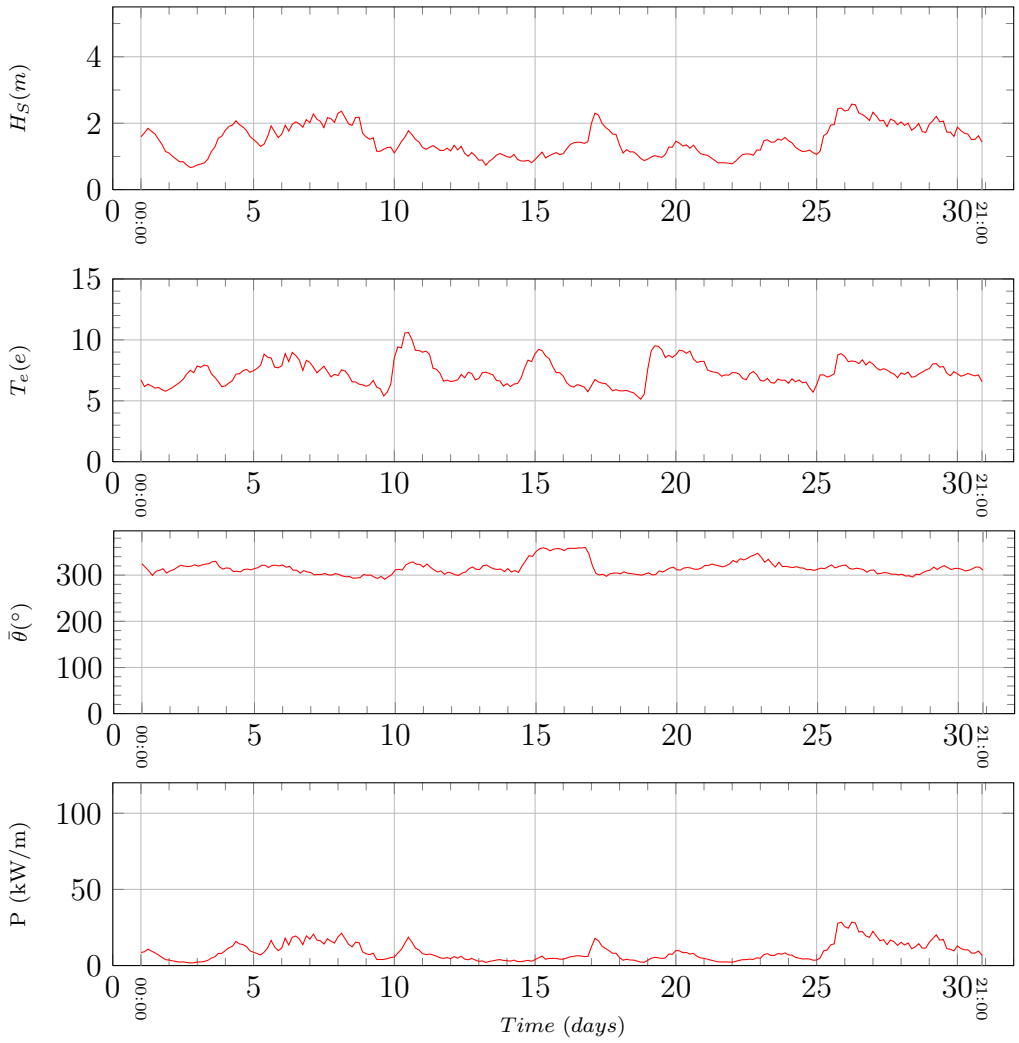


Figure 4: Wave parameters and power obtained from buoy measurement in the Pilot Zone (see Figure 3): observed $H_S$, $T_e$ and $\bar{\theta}$, for June 2008.

### 4.2.2 October 2008

Direction ($\bar{\theta}$) is in accordance to nautical convention, and must be measured counter-clockwise starting from North (North axis $\equiv 360°$). October, as expected, is a more energetic month. Wave heights peaks up remarkably (days 22nd and 29th). Confront with Figures 25 to 27, in section 8.1.

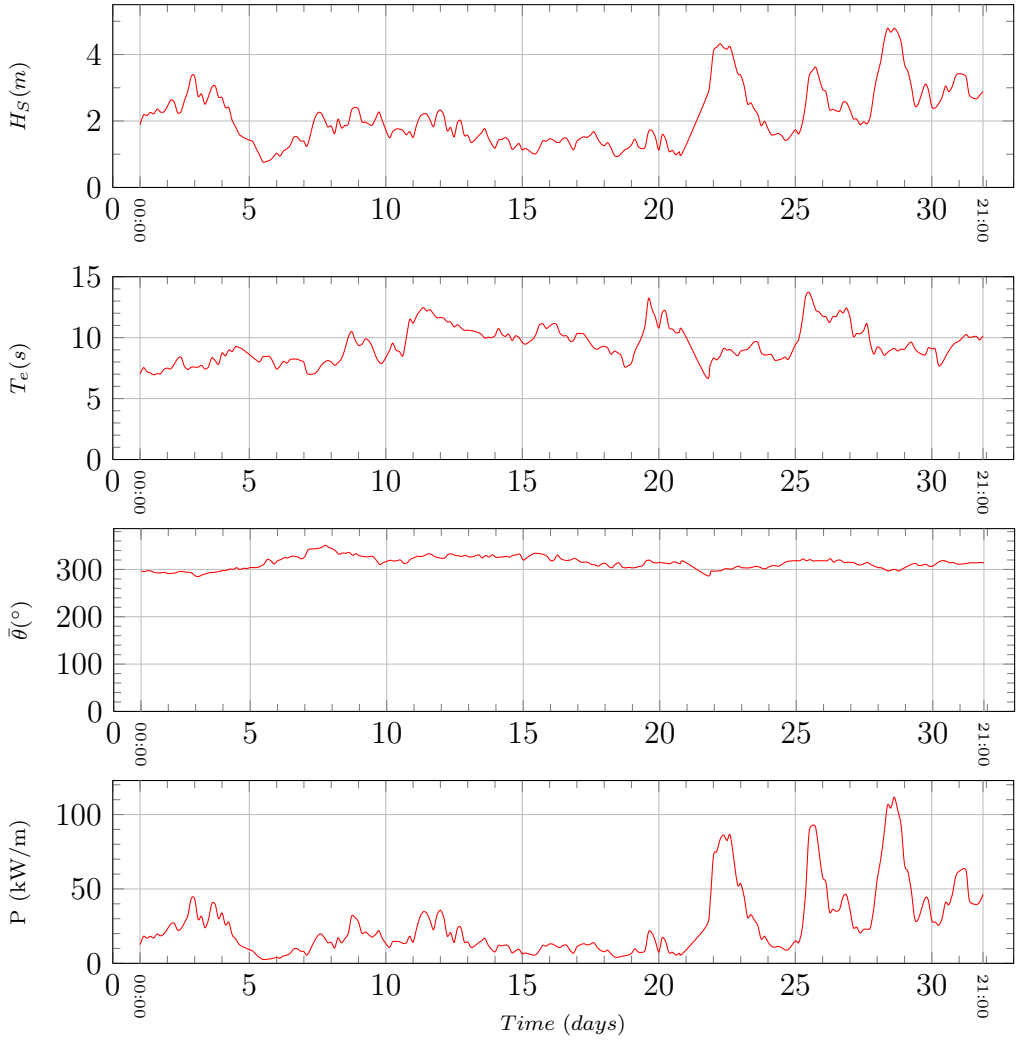


Figure 5: Same as Figure 4, for October 2008.

## 4.3 WAM and Mar3G: time-series

MAR3G, developed at the Institute of Meteorology and in operational use since 1996, is a deep water third-generation wave model (that is coupled to a inverse-ray refraction model for the nearshore are) and includes a parameterization for the effect of wind variability on the Miles mechanism for wave generation and development, which improves significantly the model performance.

Directional spectra, described into 25 frequency and 24 direction bands, are calculated at each grid point, and consequently descriptive parameters of the sea state are calculated, such as significant wave height ($H_s$), mean wave direction and wave energy period ($T_e$).

For coastal areas, MAR3G is linked to a Inverse-ray refraction model, which reproduces the effects of shoaling, refraction, shelter by the coastline and dissipation by bottom friction [Pires, 1993].

Wave parameters obtained from MAR3G have been previously used as boundary conditions for SWAN model for the same are (Pilot Zone) showing reasonably accuracy except for energy period $T_e$. [Bruck et al., 2009]. Therefore, new boundary conditions (WAM model results) have been arranged and used as boundary conditions to SWAN model.

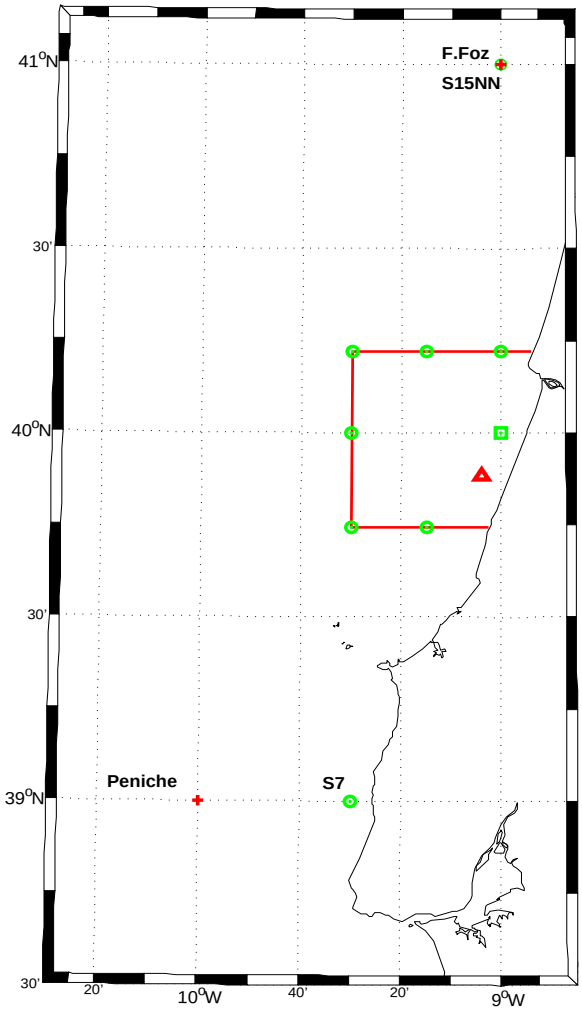


Figure 6: Location of MAR3G grid nodes (red crosses) and WAM nodes (green dots), buoy (triangle), 2D WAM spectra prescribed (except the one lying inside the box, marked with a squre) at SWAN boundaries (box). Both stations at the very North (F. Foz and S15NN) have same co-ordinates; stations in the South (Peniche and S7) are distanced by some 40 km.

### 4.3.1 June 2008

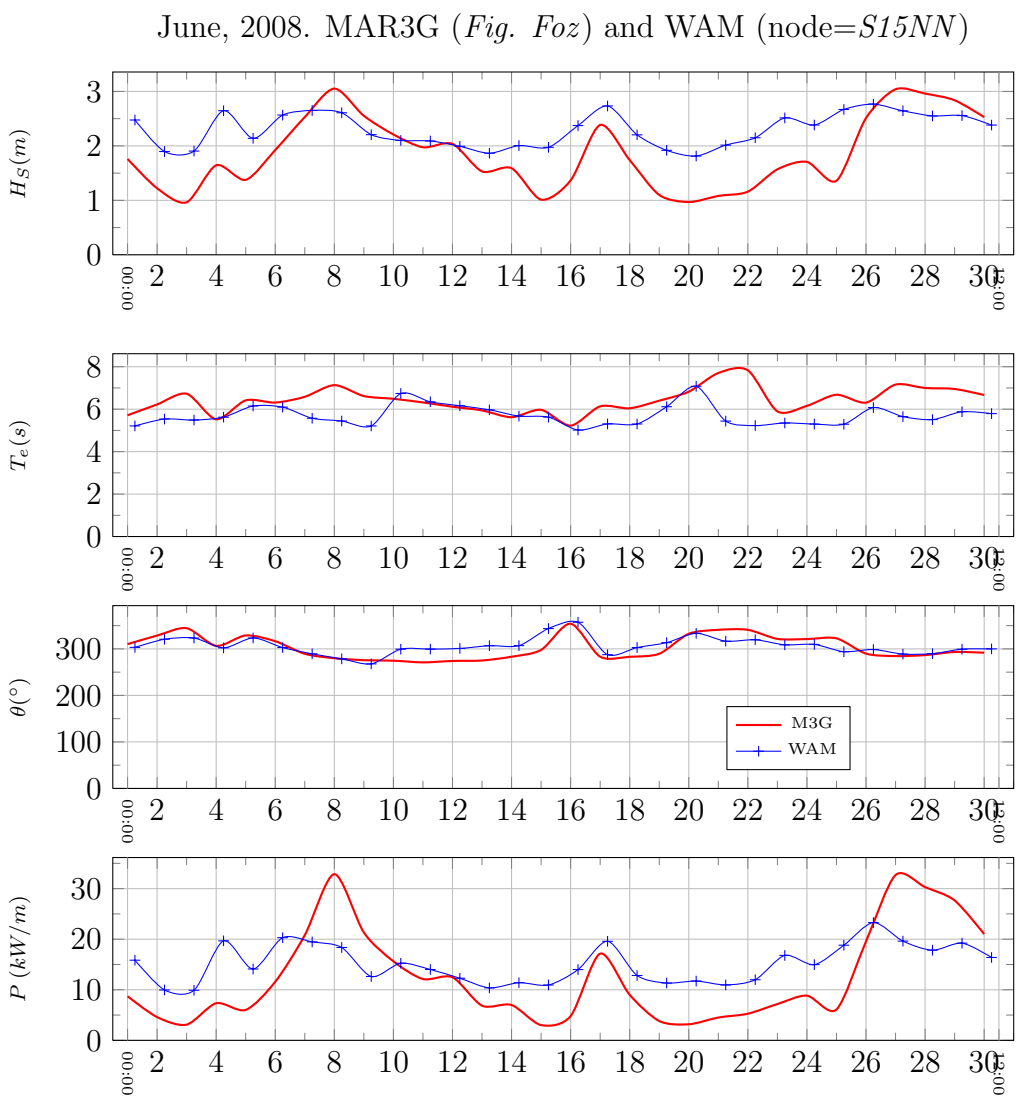


Figure 7: Comparing WAM and MAR3G wave parameters. Both nodes, located at same coordinates (41°N, 9°W) and water depth = 82 meters, June 2008.

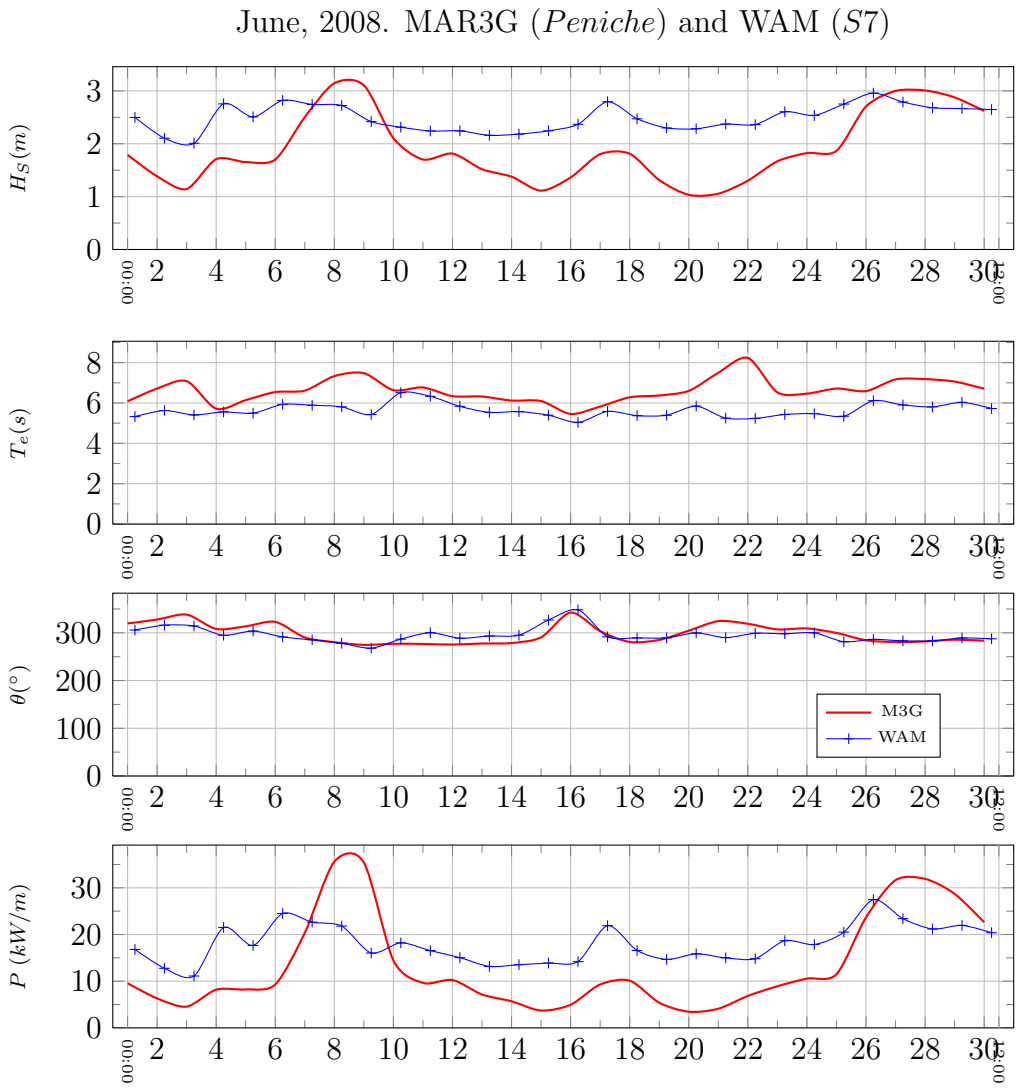


Figure 8: Comparing WAM's and MAR3G's wave parameters. *S*7 (39°N, 9.5°W) and *Peniche* (39°N, 10°W). Water depth is 55 (for *S*7) and 245 (for *Peniche*) meters, June 2008.

### 4.3.2 October 2008

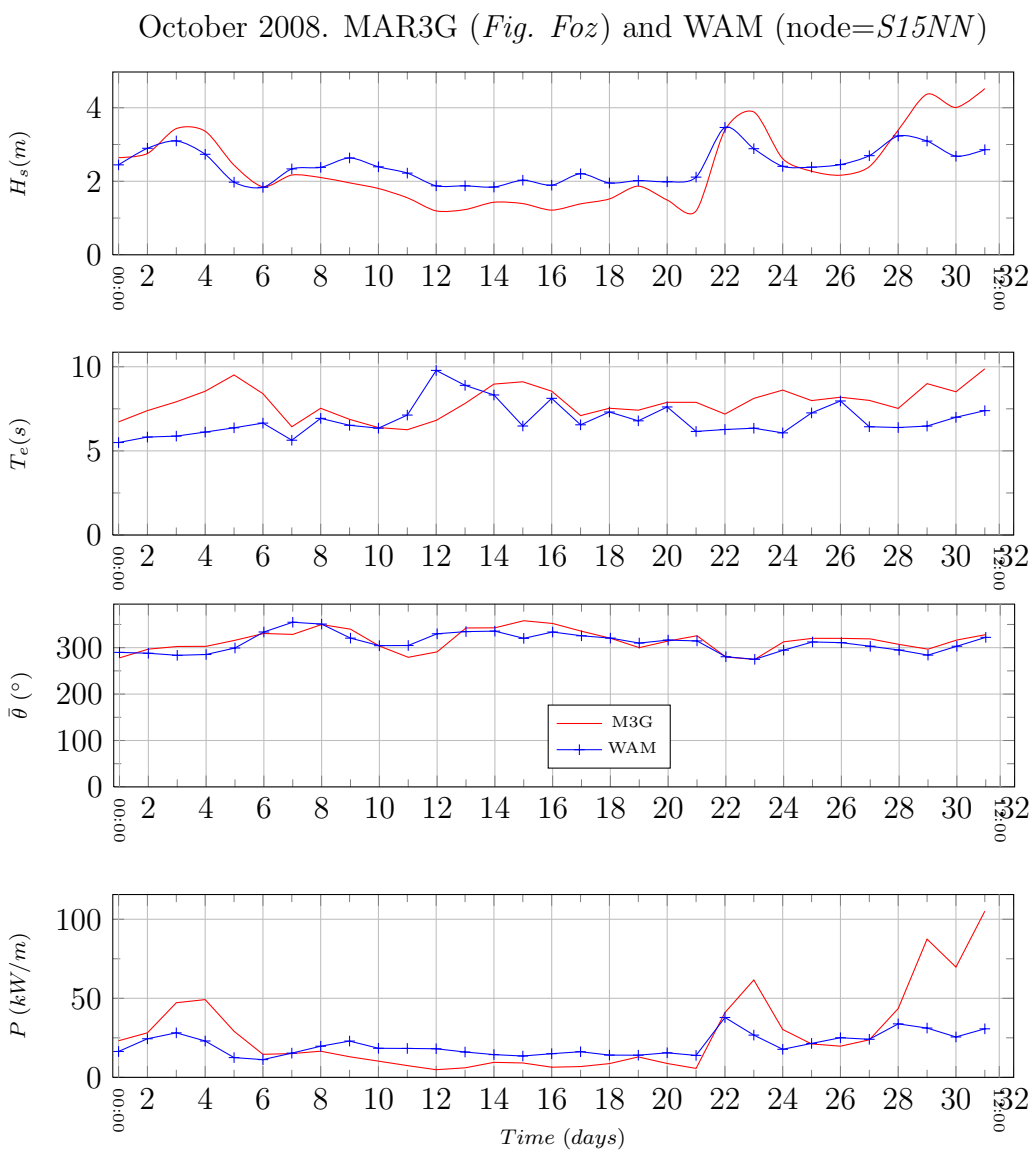


Figure 9: Same as in Figure 7, October 2008.

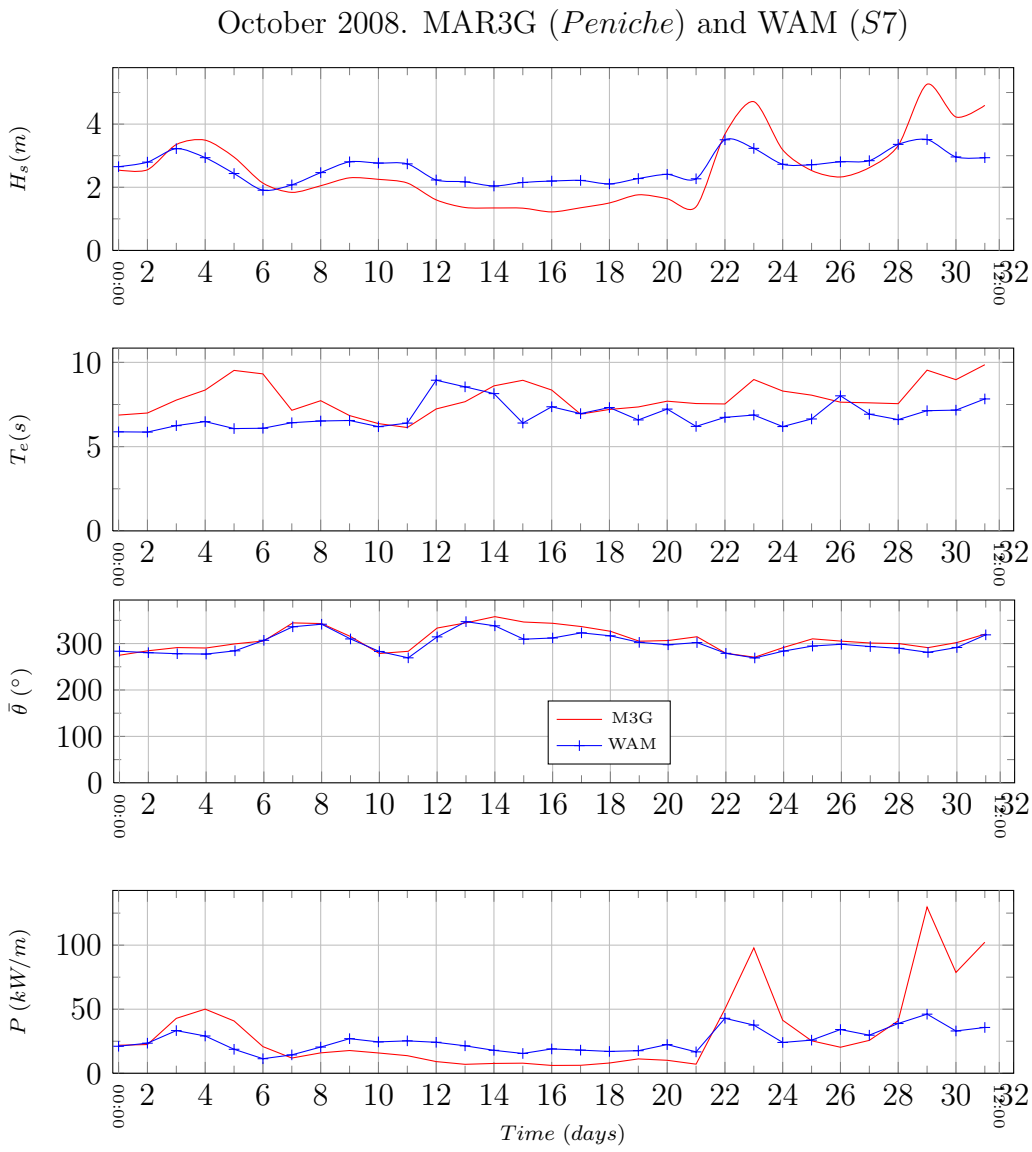


Figure 10: Same as in Figure 8, October 2008.

# 5 Forcing

## 5.1 Wind

Wind field, used for forcing SWAN, is provided by MM5 model [Grell et al., 1994] with 5 km × 5 km resolution. Temporal resolution is 3 hours. Nevertheless, for sake of time-frames consistency with WAM boundary conditions, wind forcing time-step has been increased[3] to 6 hours.

The MM5 wind field was defined over equally-spaced grid-points along x-direction ($\Delta x$ constant), while it was given along **non** equally-spaced y nodes ($\Delta y$ increases with latitude[4]). According to SWAN specification, each field must be prescribed as a regular, uniform and equally spaced grid. This problem has been overcome by creating[5] a new grid that differs in grid spacing. In fact, for this interpolated field, $\Delta y$ is constant over latitude.

In conclusion, wind forcing is prescribed over the whole computational grid, with a constant 5 km×5 km spatial resolution and 6 hours time step.

### 5.1.1 Wind Data Verification

With the purpose of assessing eventual discrepancy between wind input (the wind field provided by MM5) and wind output (SWAN output), SWAN was requested to print field values (both $u$ and $v$ components) at buoy's location. Results of MM5 wind field and SWAN where thus compared with wind input: they match perfectly. This test has been run in both stationary and non stationary mode and **ensures that wind has been properly red**.
Following plots show the match between wind input and output for both wind magnitude and wind direction.

### 5.1.2 Wind magnitude and modelled wave height

Peaks in wave height (Hs) are strongly influenced by wind field: significant stormy events (denoted by letter $S$ in Figure 11) influence, presumably, *extreme* wave heights. Wind input, rather than boundary conditions, seems thus to be the dominant driver for extreme values; conversely, under normal (non stormy) conditions relation to boundary conditions is observed to be strongest.

In fact in correspondence of those peaks (letter $S$, Figure 11), boundary condition (Hs) only show smaller bulges, or do not even show any as for the smaller peak bounded by mayor peaks in Figure 11, whilst wind magnitude ($\|\vec{v}\|$) does show, there, an abrupt

[3] by merely skipping even time-steps from the list containing wind filed as a function of time, see [Team, 2008]

[4] Mercator projection, the standard defining for geo-referencing wind filed, is not equally spaced over latitude.

[5] New field has been interpolated employing MatLab's *interp2* function. Method for interpolation is cubic spline.

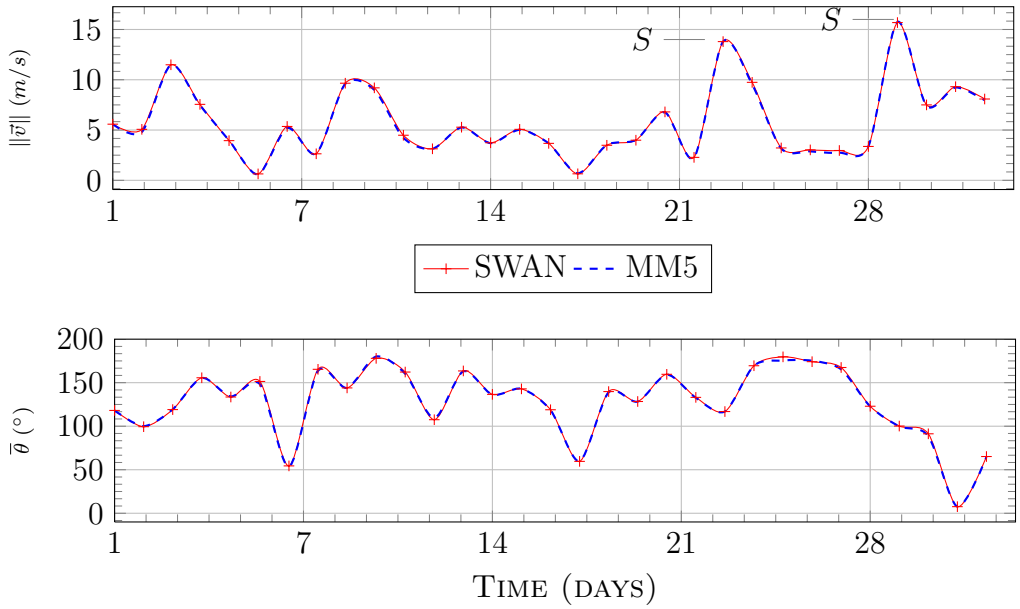


Figure 11: Comparing SWAN and MM5 wind magnitude (upper panel) and nautical direction (lower panel), at buoy site, October 2008: wind data are assimilated properly. Stormy events are represented by letter $S$. For both models: $\Delta$t=6 hrs.

increment.

What follows (Figure12) is the overlap of wind magnitude $\|\vec{v}\|$ at buoy position and buoy significant wave height ($H_s$), October. The lower panel shows the difference when allowing /disallowing wind forcing[6]: as mentioned above, in storms expected values ($H_s$) **increase** when wind input is switched on and **decrease** when wind is switched off. Non stormy conditions events show weaker correlation with wind profile.

[6]GEN2, all physical parameters set to their respective default value

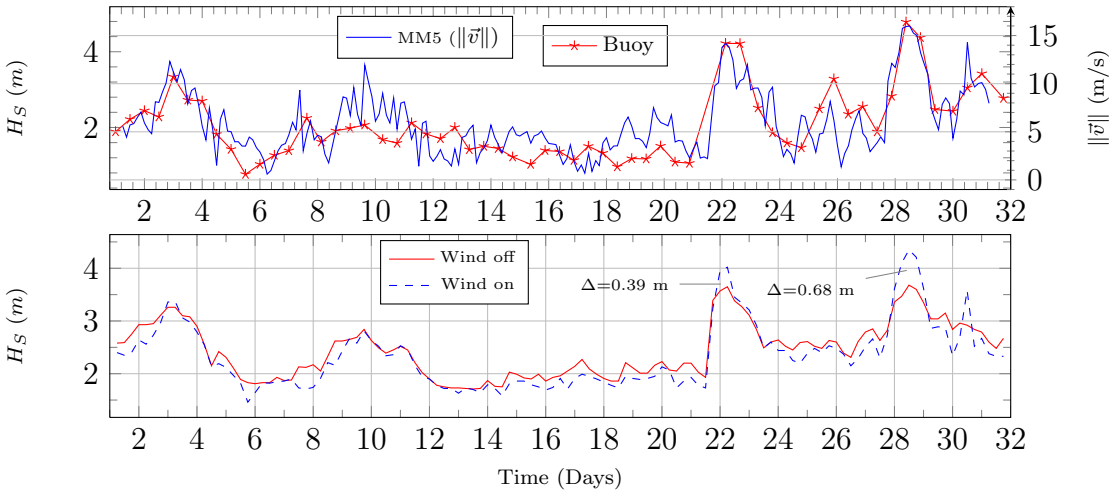


Figure 12: Comparison between MM5' wind magnitude, $\|\vec{v}\|$, and measured wave height, $H_s$ (upper panel). The lower panel shows the SWAN results obtained with wind generation option show important differences against no wind generation results at days 22 and 29, October 2008.

## 5.2 WAM Boundary Conditions

WAM 2D spectra are used for prescribing conditions at the model's boundaries. These spectra are given over a 0.25 degree grid (equally spaced along x- and y- direction) and are defined over 24 directions and 30 (non equally spaced) frequencies [Group, 1988].

Time-window covers period starting on 01/10/2008, 06:00 AM until 31/10/2008 06:00 PM, with a 6 hours time step and 01/06/2008 06:00 AM until 30/06/2008, 06:00 PM.

The boundary conditions are prescribed at the points shown in Figure 1 along the border of the computational grid: one over southern boundary ("S10N"), three along western boundary (S10, S11, S12) and two along northern boundary[7] ("S12N", "S12NN").

Water depth at the western boundary (see Figure 1) is 135 meters (S10), 119 meters (S11) and 154 meters (S12). As for northern boundary, water depth for S12N and S12NN is respectively 113 and 59 meters; for S10N (southern boundary) water is 106 meters deep. At station $S_B$ water depth is 36 meters.
Besides the spectra along boundaries, another WAM spectrum (defined on the 0.25° grid) is available in the proximity of the buoy location: $S_B$ (within a radius of approximately 10 km, cfr. with Figure 1).

[7]Spectra at the corners are prescribed over both sub-segments enclosing that corner

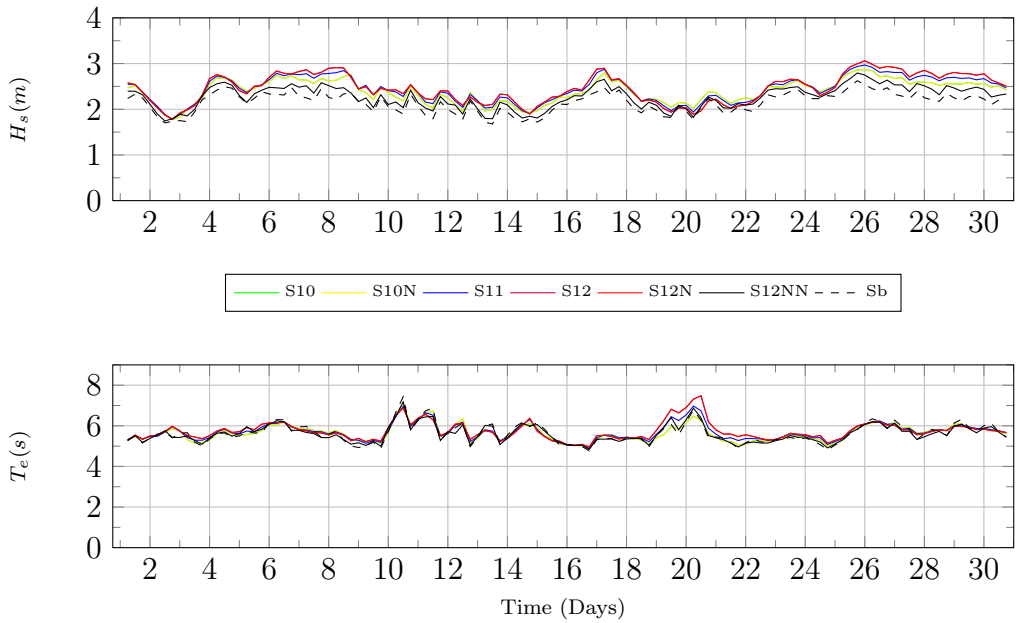


Figure 13: Comparison of $H_S$ and $T_e$ WAM results at the boundaries, June 2008. Hs (top), Te (bottom) for each station on the grid, including $S_B$ (the one located next to the buoy). The values of $T_e$ are very similar at all boundary points where WAM results are prescribed as SWAN boundary conditions.

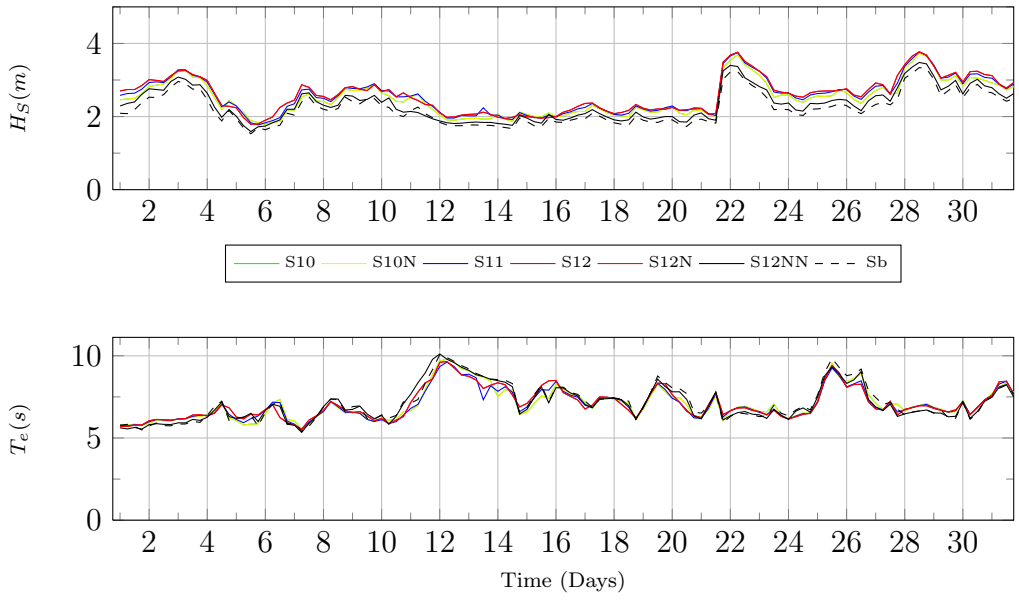


Figure 14: Same as in Figure 13, October 2008.

# 6 Results obtained with SWAN model

This section presents the results obtained with SWAN wave model for months June and October.
SWAN model has been run in nonstationary $3^{rd}$ generation mode (KOMEN wind Scheme). Figure 16 presents the comparison of SWAN results at buoy location, buoy data and also WAM results.
Error statistics are reported in Tables 1 and 2, respectively for Buoy-SWAN and Buoy-WAM.

## 6.1 June

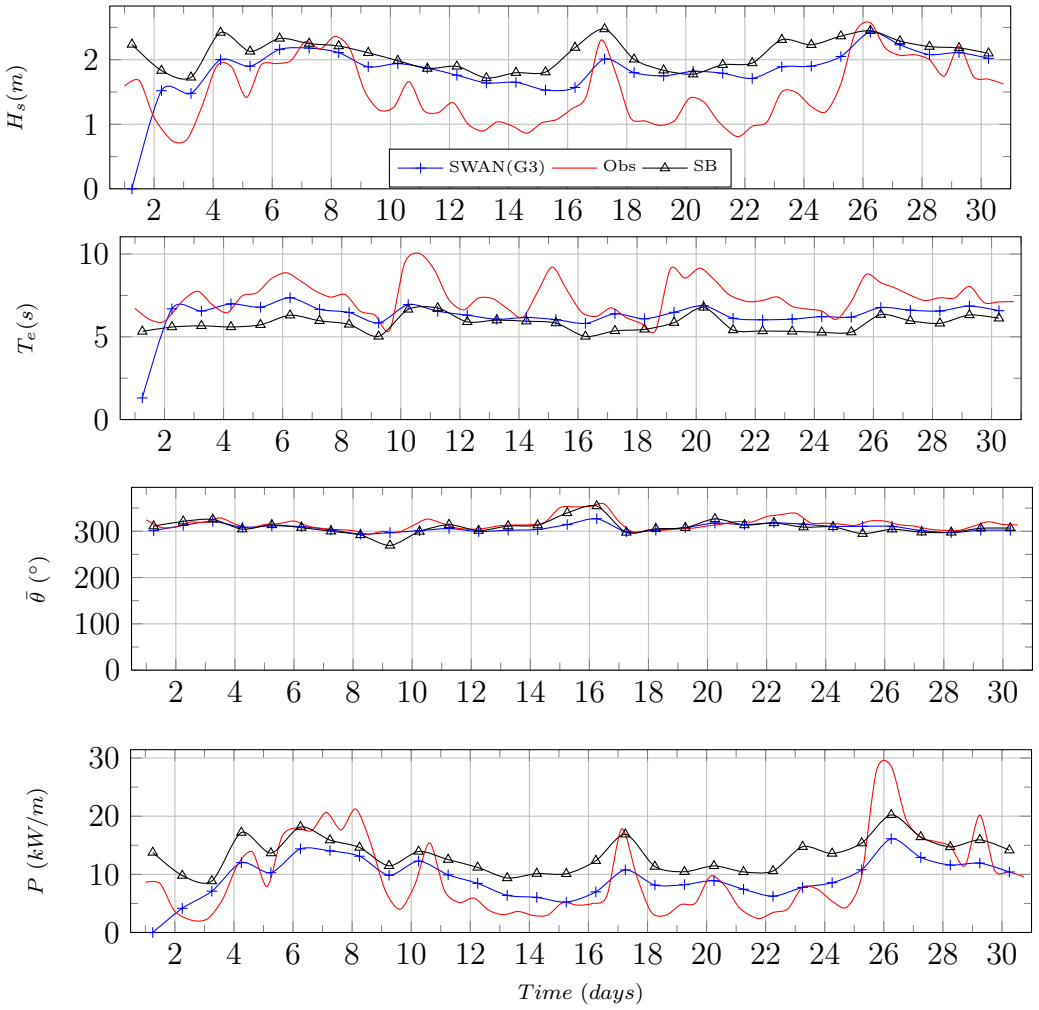


Figure 15: Comparison of SWAN results (—+—) at buoy location to buoy data (——), and also WAM results (—△—) at station $S_B$ (see Figure 1), June 2008.

## 6.2 October

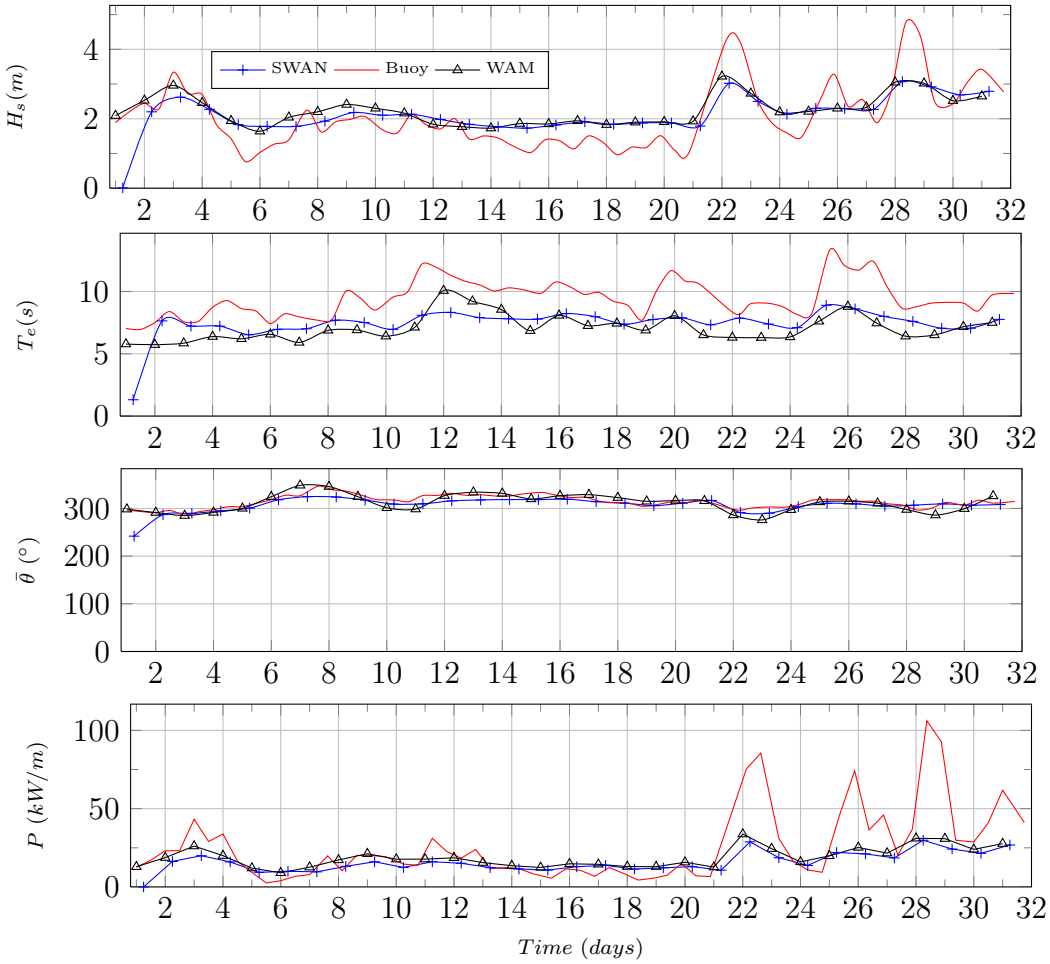


Figure 16: Comparison of SWAN results (—+—) at buoy location to buoy data (——), and also WAM results (—△—) at station $S_B$ (see Figure 1), October 2008.

The above figure shows that, except for for $T_e$, WAM and SWAN results are almost coincident, which means that shallow water phenomena taken into account by SWAN do not cause significant modifications in the wave parameters (height and direction). However, these results show important differences in wave height when compared to buoy data.
On what concerns Te, SWAN results are different (either larger and smaller) of WAM results; SWAN underpredicts buoy data, which also happens with MAR3G results (see Section 4.3).

It has to be stressed that WAM, SWAN and buoy $\bar{\theta}$ are almost coincident.

## 6.3 Error Statistics

| | October | | | June | | |
|---|---|---|---|---|---|---|
| | *Bias* | $E_{rms}$ | S.i. | *Bias* | $E_{rms}$ | S.i. |
| Hs (m) | -0.05 | 0.34 | 0.27 | -0.38 | 0.27 | 0.28 |
| Te (s) | 1.86 | 4.78 | 0.28 | 0.91 | 1.76 | 0.20 |
| $\overline{\theta}$ (°) | 6.16 | 98.51 | 0.03 | -1.12 | 98.46 | 0.10 |
| Power (kW/m) | 4.83 | 197.31 | 1.74 | -0.18 | 7.54 | 0.57 |

Table 1: Error Statistic, SWAN model vs. Buoy, October and June 2008.

| | October | | | June | | |
|---|---|---|---|---|---|---|
| | *Bias* | $E_{rms}$ | S.i. | *Bias* | $E_{rms}$ | S.i. |
| Hs (m) | -0.13 | 0.28 | 0.25 | -0.67 | 0.55 | 0.50 |
| Te (s) | 2.28 | 5.96 | 0.25 | 1.69 | 3.42 | 0.25 |
| $\overline{\theta}$ (°) | 1.89 | 125.55 | 0.03 | -2.10 | 145.49 | 0.12 |
| Power (kW/m) | 3.27 | 158.63 | 1.30 | -2.29 | 17.91 | 0.61 |

Table 2: Error Statistic, WAM model vs. Buoy, October and June 2008.

## 6.4 Power Exceedance

This section is dedicated to present power exceedance. Exceedance directly describes the waves energy contents of wave power, i.e. the percentage of time wave power exceeds each power level.

Exceedance has been calculated for data-set relative to **(a)** buoy data, **(b)** SWAN simulations and **(c)** WAM simulations.

Buoy data show more energetic conditions.

### 6.4.1 June 2008

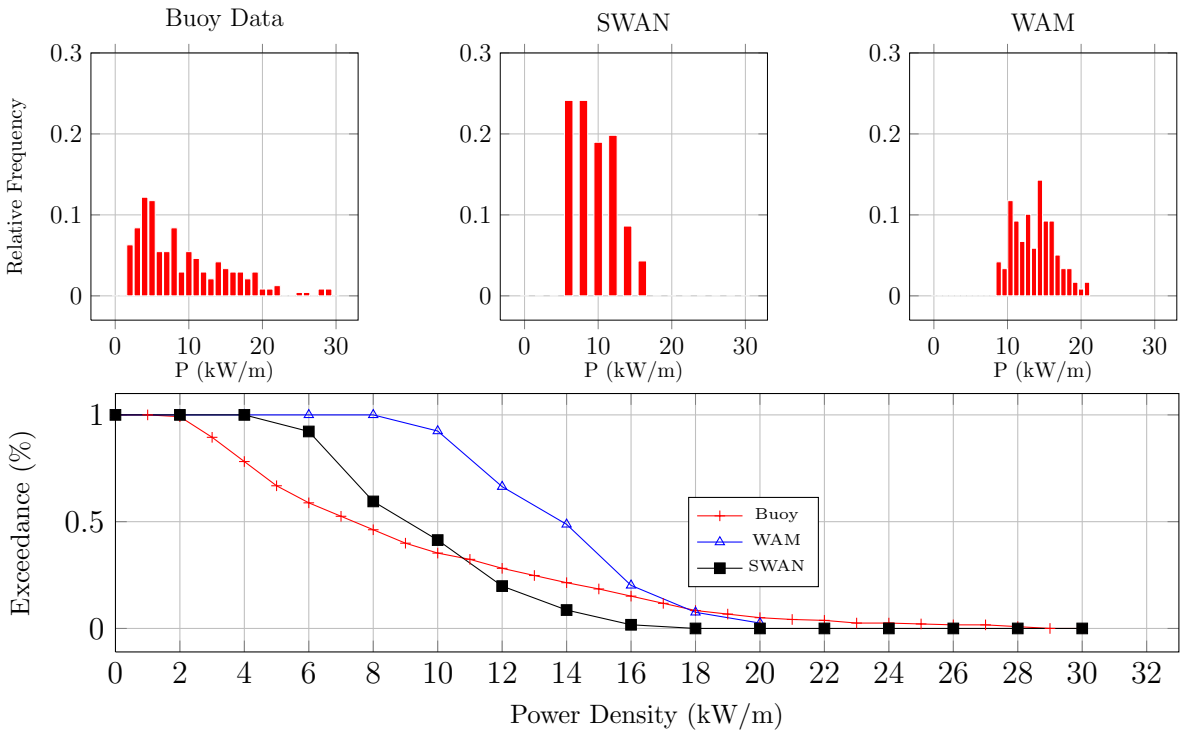


Figure 17: Representation of power resource, for SWAN, WAM (station $S_B$) and buoy data at buoy site, October 2008. Top: histograms of relative frequency. Bottom: Exceedance curves.

### 6.4.2 October 2008

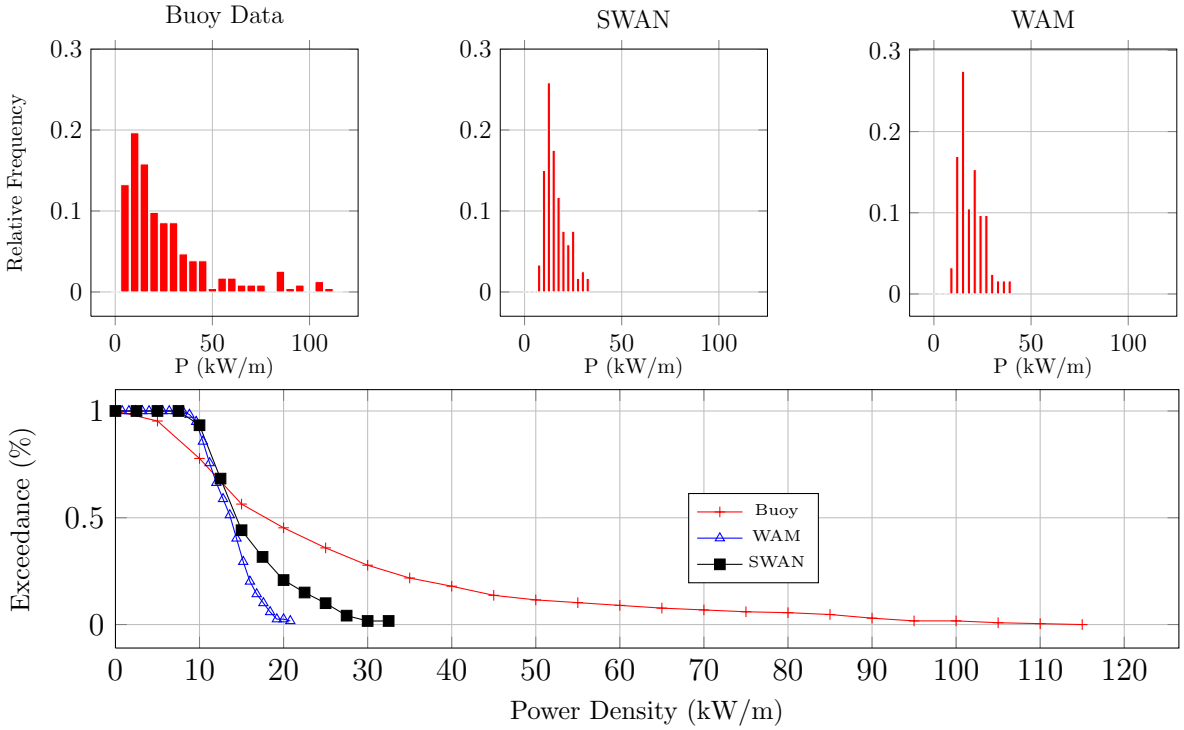


Figure 18: Representation of power resource, for SWAN, WAM (station $S_B$) and buoy data at buoy site, October 2008. Top: histograms of relative frequency. Bottom: Exceedance curves.

# 7 WAM and Mar3G 1D Spectra

## 7.1 Figueira da Foz

Following figures (19 to 21) represent comparison of $WAM$ - $MAR3G$ one dimensional spectra ($S(f)$) for month of October (**left columns**) and June (**right columns**), station tagged as "*Figueira da Foz*" (see Figure 6).

Station compared are **both** located at following co-ordinates: 41°N, 9°W.

As observed with other comparisons (in situ and WAM 1D Spectra), WAM model remarkably underestimates wave parameters for more energetic sea states.

Discrepancy increases when $S(f)$ increases: most energetic condition are underestimated by the models.

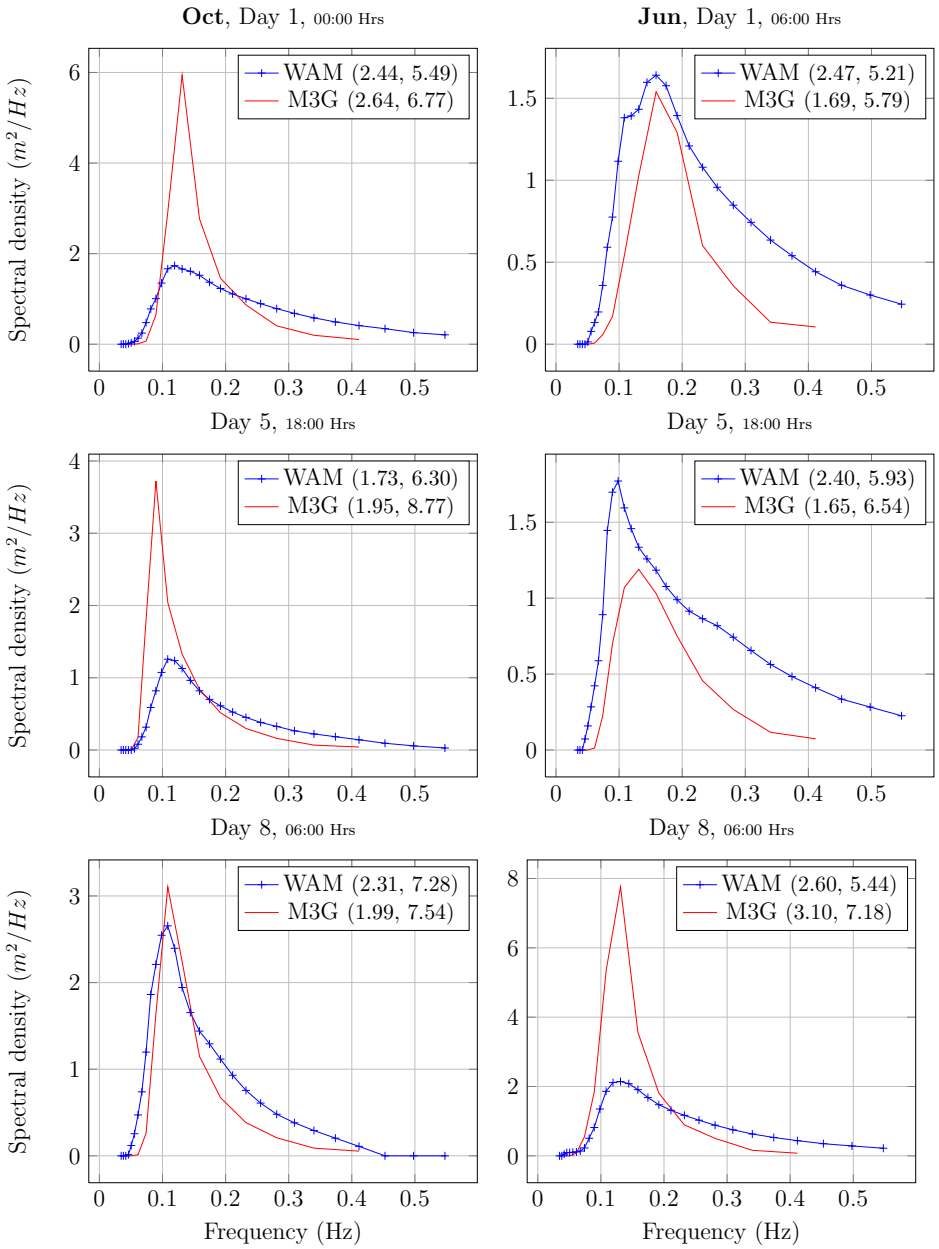


Figure 19: Overlapping simulations (WAM station S15NN) and MAR3G 1D spectra *Figueira da Foz*. Left column represents October, right one June. Pair of numbers (legend) report, respectively, Hs (m) and Te (s) for each curve.

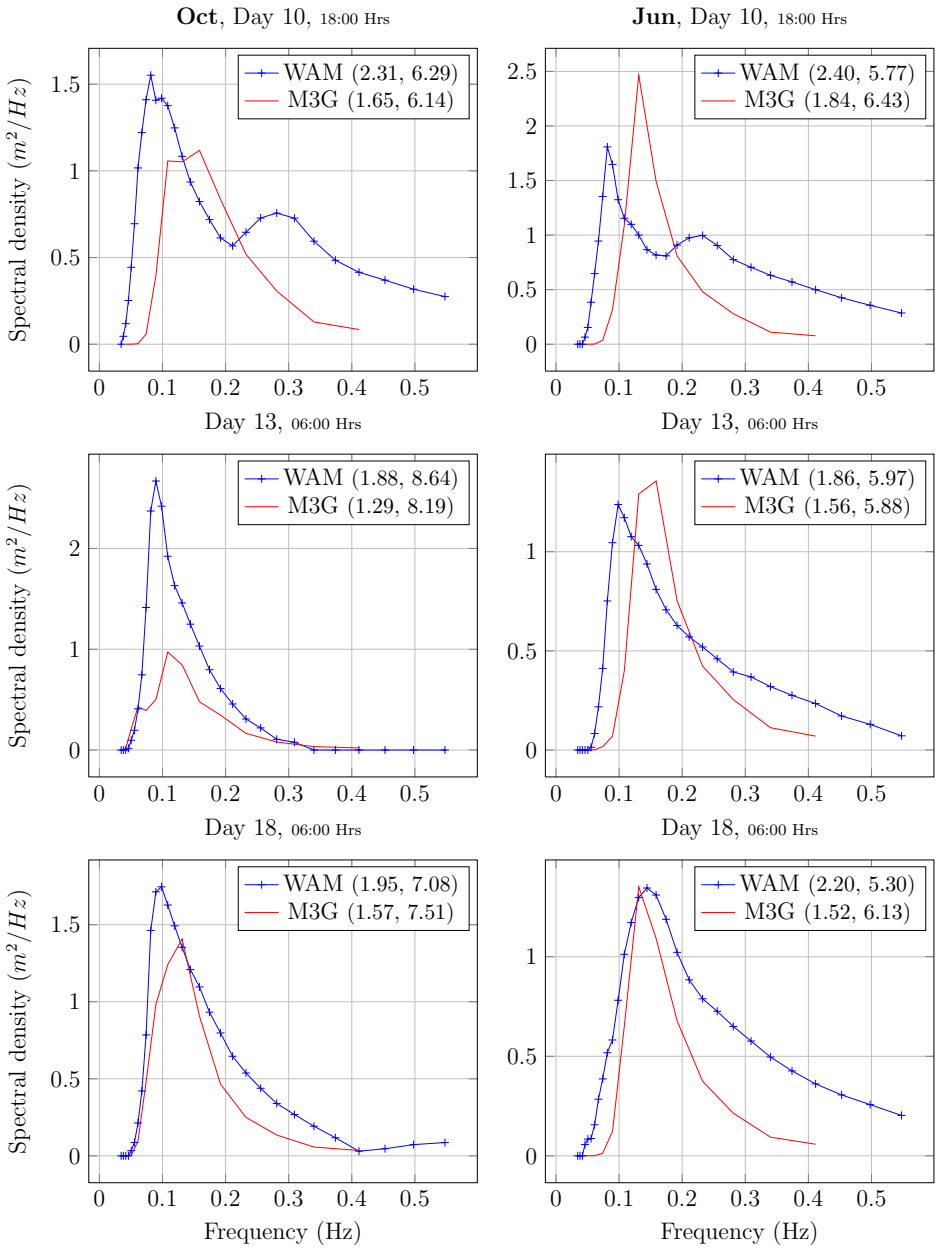


Figure 20: Overlapping simulations (WAM station S15NN) and MAR3G 1D spectra, *Figueira da Foz*. Left column represents October, right one June. Pair of numbers (legend) report, respectively, Hs (m) and Te (s) for each curve.

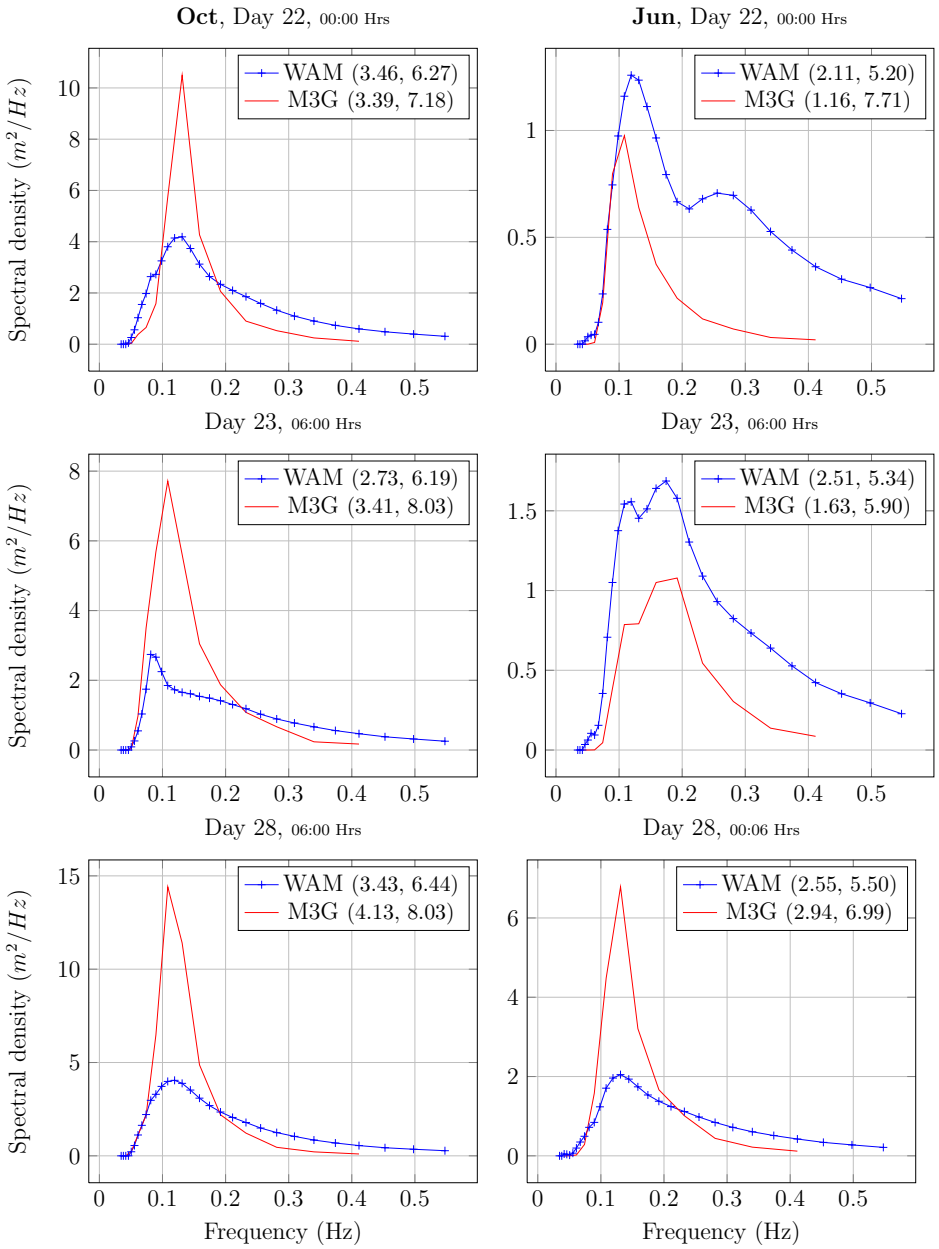


Figure 21: Overlapping simulations (WAM station S15NN) and MAR3G 1D spectra *Figueira da Foz*. Left column represents October, right one June. Pair of numbers (legend) report, respectively, Hs (m) and Te (s) for each curve.

## 7.2 Peniche

Following figures (22 to 24), represent same comparison as above but for another Station: "*Peniche*". In this case, $WAM$ and $M3G$ stations do not have the same coordinates: they are some 43 $km$ far away from each other.

$M3G$ node, tagged with coordinates (66 20), is located at following coordinates: 39°N, 10°W (water depth=248 meters).
$WAM$ node is located at 39°N, 9.5°W (water depth $\approx$ 45 meters)

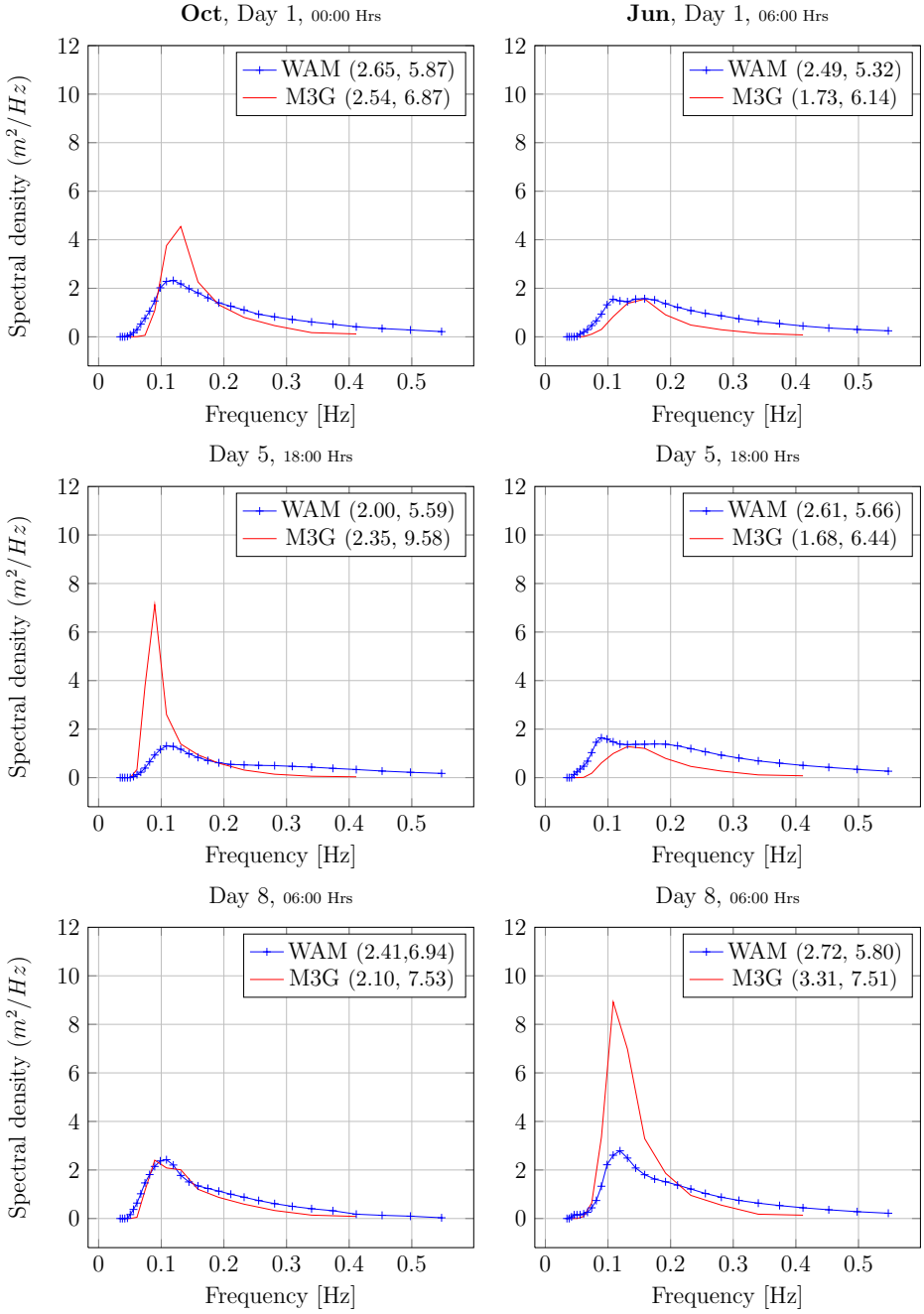


Figure 22: Overlapping simulations (WAM station S7) and MAR3G 1D spectra (*Peniche*). Left column represents October, right one June. Pair of numbers (legend) report, respectively, Hs (m) and Te (s) for each curve.

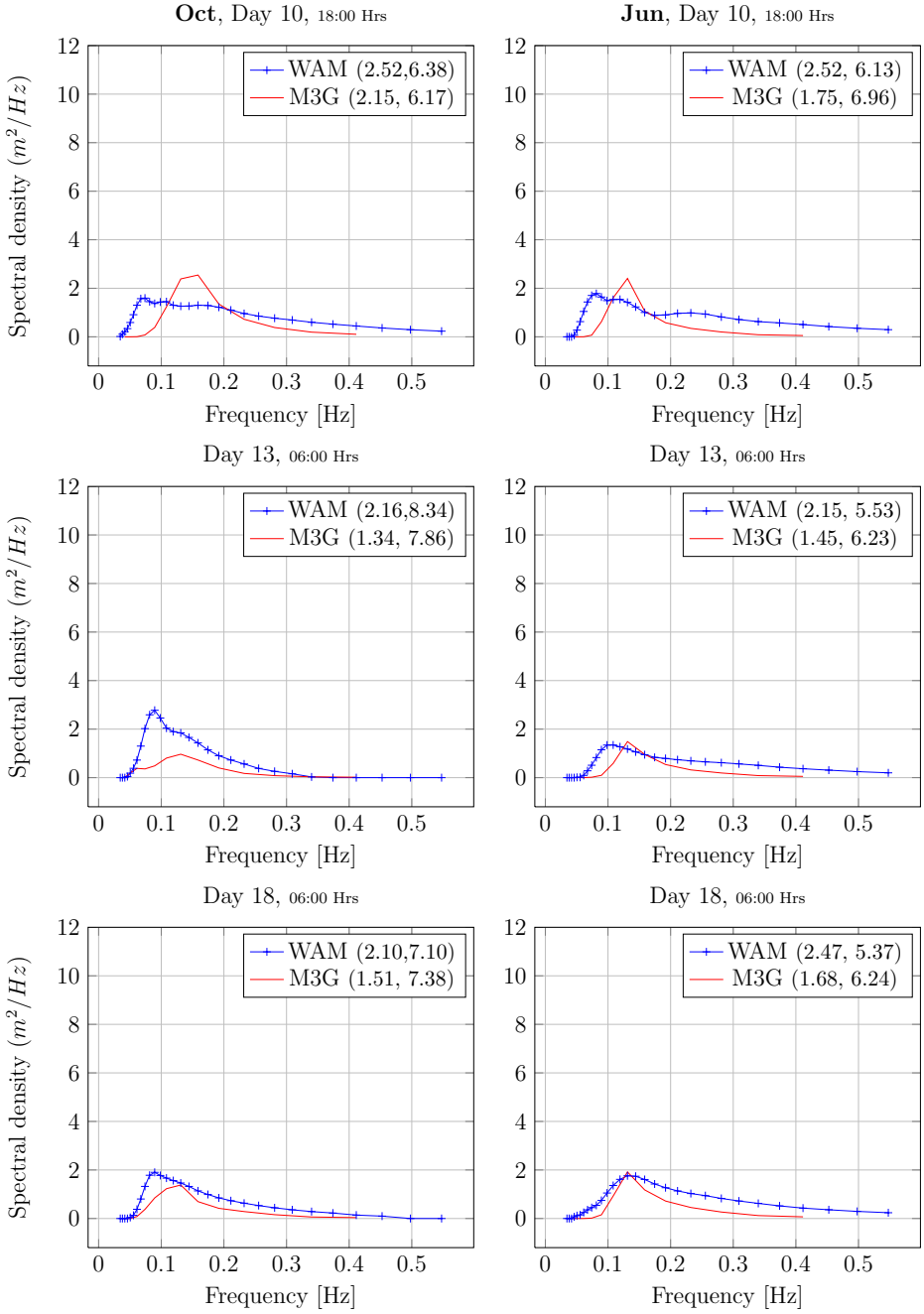


Figure 23: Overlapping simulations (WAM station S7) and MAR3G 1D spectra (*Peniche*). Left column represents October, right one June. Pair of numbers (legend) report, respectively, Hs (m) and Te (s) for each curve.

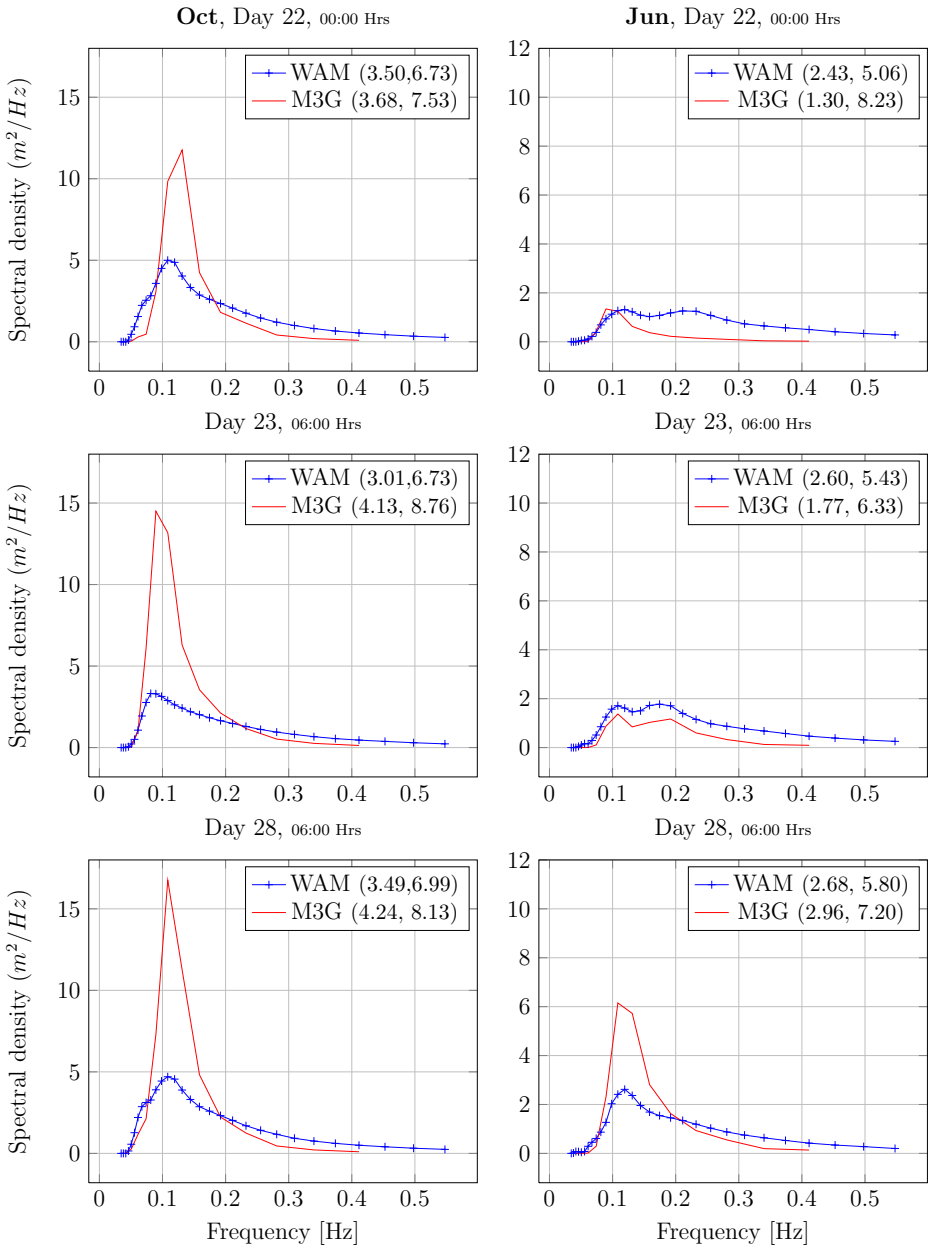


Figure 24: Overlapping simulations (WAM station S7) and MAR3G 1D spectra (*Peniche*) Left column represents October, right one June. Pair of numbers (legend) report, respectively, Hs (m) and Te (s) for each curve.

# 8 Conclusions and Future Investigations

## 8.1 Visually Inspection of Wave Spectra

In order to better understand why energy period is underestimated, **1D** input spectra (WAM, station SB, the one closest to buoy) and 1D measurements (*in situ*) have been overlapped and visually inspected. Left column shows month of October; right column (milder conditions) reports summer values.

Each subplot reports a couple of numbers, within bracket, for each of the two represented curves: they are significant wave height ($H_s$, in meters) and energy period ($T_e$, in seconds). Dates are indicated on top of each subplot.

By observing the plots (Figures 25 to 27) it is clearly evident that winter met-ocean conditions are more energetic, if compared to summer: former attains values (peaks) as high as **32** $m^2/Hz$, while latter rarely exceeds 3 $m^2/Hz$. For this milder summer conditions, discrepancies are quite small, and both curves do match. Surprisingly, extreme winter met-ocean conditions are underestimated by WAM wave model: **the gap is observed to be as high as 28** $m^2/Hz$ (see day 25/10 18:00 Hrs: Figure 27, bottom left). **It seems that WAM model cannot properly estimate extreme events, whilst low energy sea states are well predicted**.

WAM wave spectra are particularly dense for higher frequencies (Figures 25 to 27), when compared with buoy measurements. This allocation of energy in higher frequencies (i.e. lower periods), might probably be responsible for underestimation of $T_e$: simulated frequency bands (WAM) are denser than they should actually be (observations).

The fact that Hs ($=4\sqrt{(m_0)}$) is (fairly) well predicted and Te ($=m_{-1}/m_0$) is underestimated might interpreted as follows:
wave height depends *solely* on zero order moment; energy period depends on both $m_0$ and $m_{-1}$ momenta:

$$m_0 = \int_{f_{min}}^{f_{max}} \overbrace{f^0}^{=1} \, S(f)\, df \tag{13}$$

$$m_{-1} = \int_{f_{min}}^{f_{max}} \underbrace{f^{-1}}_{\neq 1} \, S(f)\, df \ . \tag{14}$$

Observed and simulated $H_s$ return, approximately, same value reflecting the **lack of dependency** of spectral *shape*.
Observed and simulated $T_e$ show remarkably divergences, **reflecting the dependency on spectral *shape***.
WAM spectral density is greater at higher frequencies ($\equiv$ lower periods): causing simulated period to be *dragged down*.
$T_e$ is a typical (spectral) asymmetry indicator, $H_s$ is not. Former is, therefore, better estimated, latter is not.

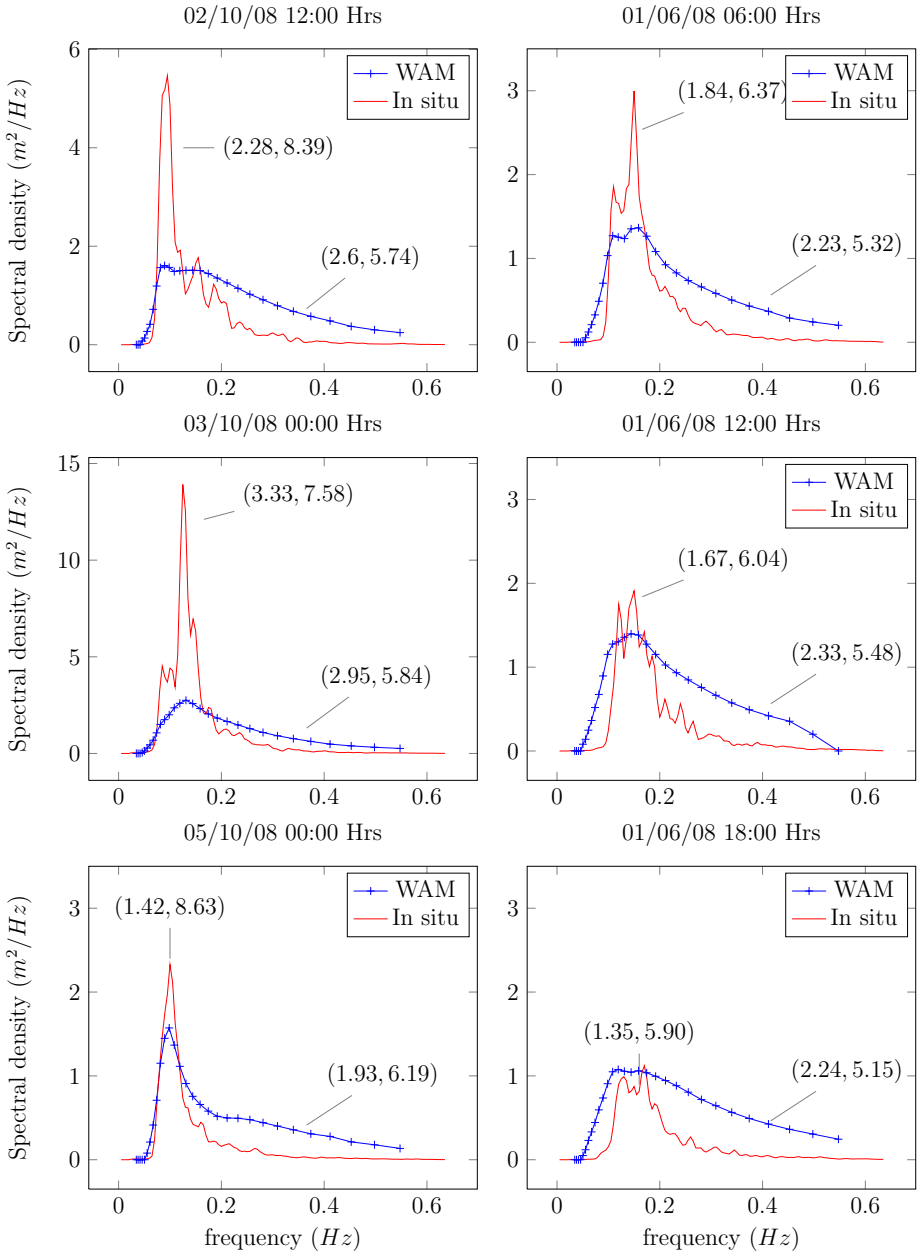


Figure 25: Overlapping simulations (WAM station $S_B$) and observations (buoy) 1D spectra. Left column represents October, right one June. Pair of numbers in each plot represent, respectively, $H_s$ (m) and $T_e$ (s) for each spectrum.

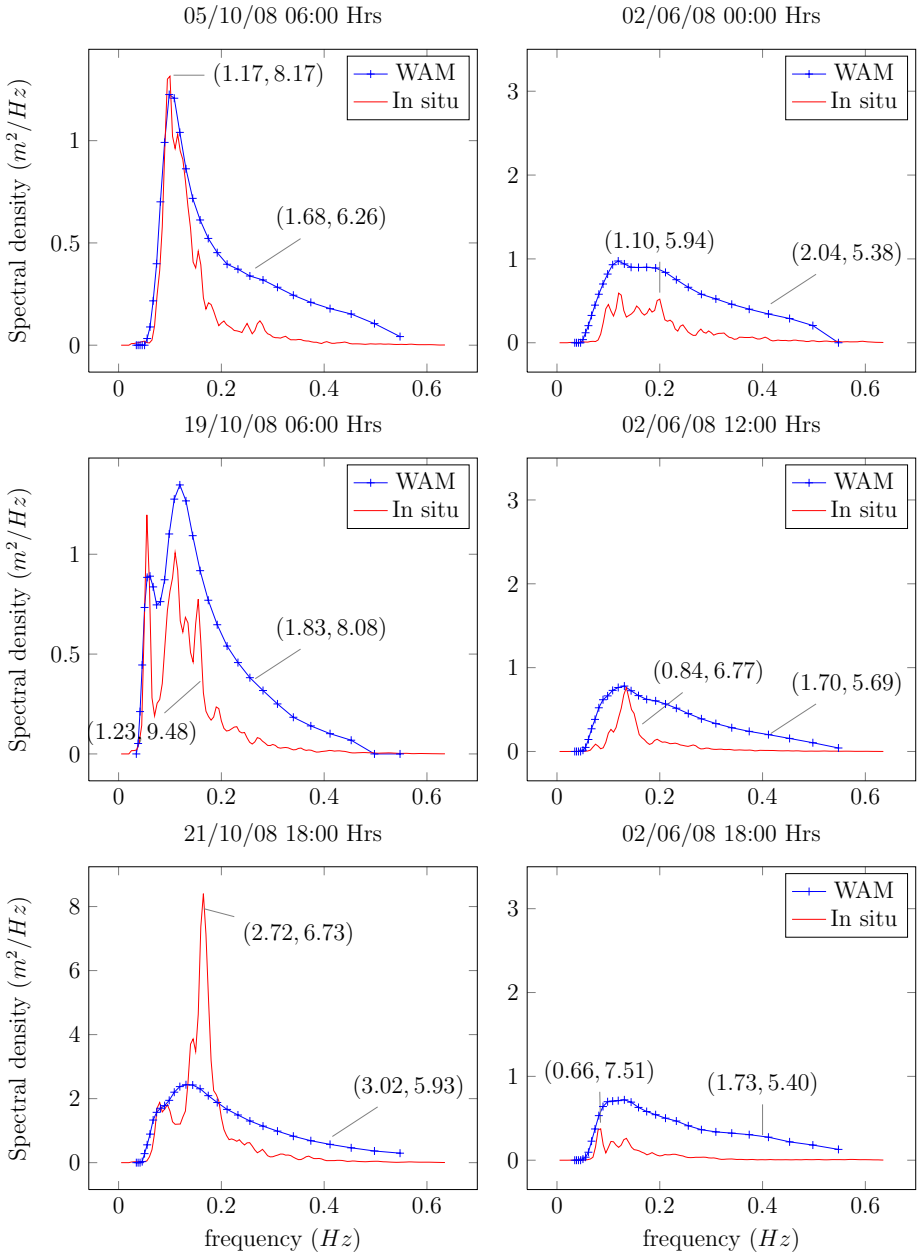


Figure 26: Same as in Figure 25.

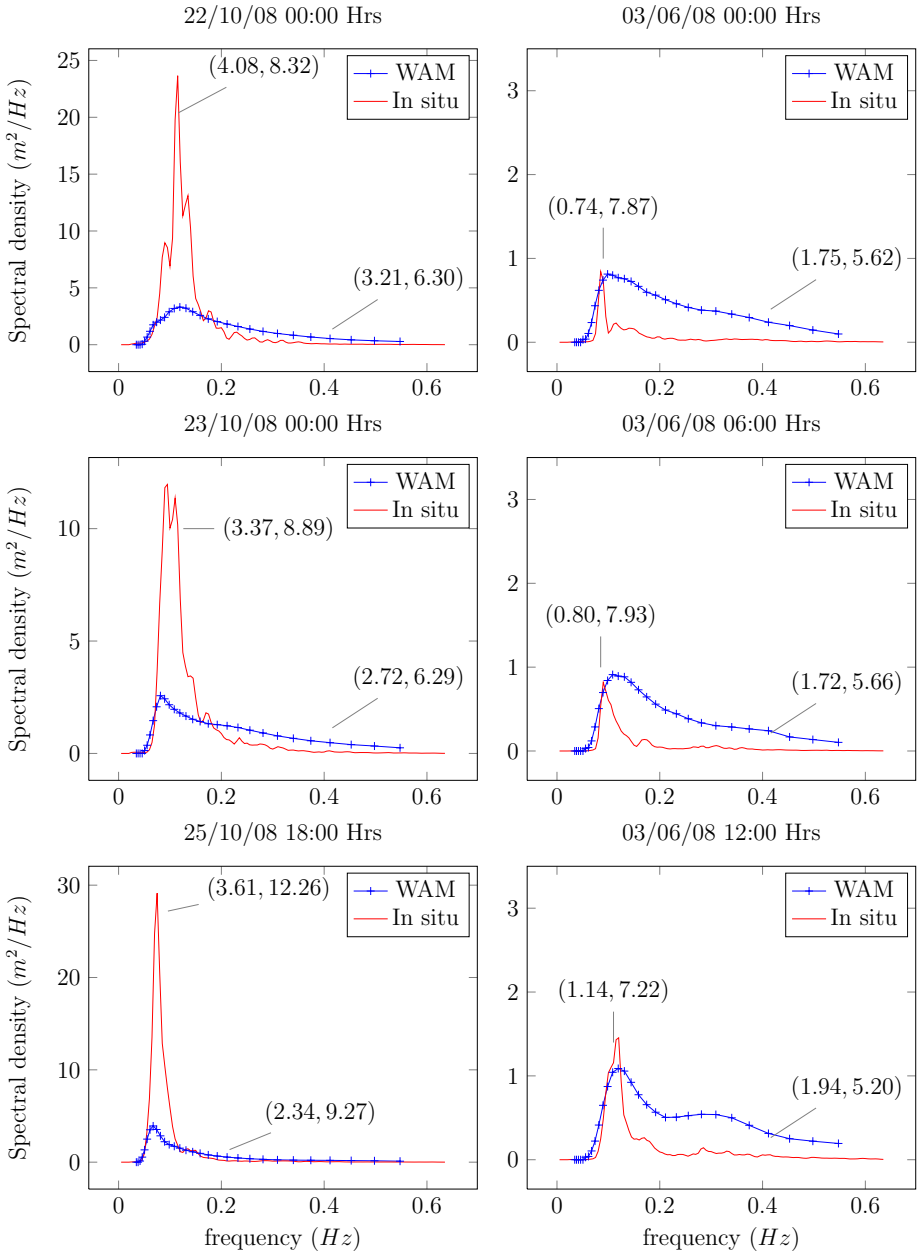


Figure 27: Most energetic occurrences for month of October (left column). Day 25-Oct at 18:00 Hrs (bottom left), shows a "jump" as high $\approx 25\ m^2/Hz$. Confront with Figure 25.

## 8.2 Discussion

In order to obtain realistic and reliable results, forcing prescribed at model's boundary must also be realistic, i.e., representing properly met-ocean conditions. It has been observed that for both models, WAM and MAR3G, this does not happen: energy period, $T_e$, is underestimated.

For this reason, I conclude that, for this special case, results are poor because forcing at boundary is (surprisingly) inappropriate, especially for more intense met-ocean conditions.

Once provided *proper* boundary conditions, a future recommendation might be (fine) tuning of parameters. Buoy is located in intermediate-depth waters: dominant factors for this case might, therefore, be related to dissipation phenomena typical for deep waters: white-capping.

# References

N. Booij, R. C. Ris, and Leo H. Holthuijsen. A third-generation wave model for coastal regions - 1. model description and validation. *Journal of Geophysical Research*, 104: 7649–7666, 1999.

M. Bruck, A. Carvalho, P. Costa, and M.T. Pontes. Joint assessment of offshore wind and wave energy resources for the portuguese pilot zone. In *Proceedings of OMAE2009 28th International Conference on Ocean*, Honolulu, Hawaii, May 31 to June 5, 2009.

Alain Clément, Pat McCullen, António Falcão, Antonio Fiorentino, Fred Gardner, Karin Hammarlund, George Lemonis, Tony Lewis, Kim Nielsen, Simona Petroncini, M. Teresa Pontes, Phillippe Schild, Bengt-Olov Sjöström, Hans Christian Sørensen, and Tom Thorpe. Wave energy in europe: current status and perspectives. *Renewable and Sustainable Energy Reviews*, 6(5):405 – 431, 2002. ISSN 1364-0321.

Datawell. Oceanographics instruments. URL `www.datawell.nl`. last access June 2009.

ECMWF. European centre for medium-range weather forecasts. URL `www.ecmwf.int`. last access September 2009.

G. A. Grell, J. Dudhia, and D. R. Stauffer. A description of the fifth-generation penn state/ncar mesoscale model (mm5). Technical report, NCAR, 1994. NCAR/TN-398+STR.

The WAMDI Group. The wam model - a third generation ocean wave prediction model. *J. Phys. Oceanogr.*, 18:1775–1810, 1988.

Leo H. Holthuijsen. *Waves in Oceanic and Coastal Waters*. Cambridge Press, 2007.

J.G. Komen, S. Hasselmann, and K. Hasselmann. *On the Existence of a fully developed sea*. Cambridge Press, 1994.

J.W. Miles. On the generation of surface waves by shear flows. *J. Fluid Mech.*, 3: 185–204, 1957.

H. Oliveira Pires. *Numerical Modeling of Wind-Generated Waves*. PhD thesis, Instituto Superior Técnico, Lisbon Technical University, 1993. (in Portuguese).

The SWAN Team. SWAN User Manual. TU-Delft, Delft, The Netherlands, 2008. SWAN Cycle 3rd version 40.72.